



OPEN

Anti-breast cancer synthetic peptides derived from the *Anabas testudineus* skin mucus fractions

Ahmed Abdul Kareem Najm¹, Ahmad Azfaralariff^{2,4}, Herryawan Ryadi Eziwar Dyari³, Babul Airianah Othman², Muhammad Shahid¹, Nahid Khalili¹, Douglas Law⁵, Sharifah Sakinah Syed Alwi⁶ & Shazrul Fazry^{2,4,7}✉

Previous study has shown the antimicrobial activities of mucus protein extracted from *Anabas testudineus*. In this study, we are interested in characterizing the anticancer activity of the *A. testudineus* antimicrobial peptides (AMPs). The mucus was extracted, fractioned, and subjected to antibacterial activity testing to confirm the fish's AMPs production. The cytotoxic activity of each fraction was also identified. Fraction 2 (F2), which shows toxicity against MCF7 and MDA-MB-231 were sent for peptide sequencing to identify the bioactive peptide. The two peptides were then synthetically produced and subjected to cytotoxic assay to prove their efficacy against cancer cell lines. The IC₅₀ for AtMP1 against MCF7 and MDA-MB-231 were 8.25 ± 0.14 µg/ml and 9.35 ± 0.25 µg/ml respectively, while for AtMP2 it is 5.89 ± 0.14 µg/ml and 6.97 ± 0.24 µg/ml respectively. AtMP1 and AtMP2 treatment for 48 h induced breast cancer cell cycle arrest and apoptosis by upregulating the p53, which lead to upregulate pro-apoptotic BAX gene and downregulate the anti-apoptotic BCL-2 gene, consequently, trigger the activation of the caspase-3. This interaction was supported by docking analysis (QuickDBD, HPEPDOCK, and ZDOCK) and immunoprecipitation. This study provided new prospects in the development of highly effective and selective cancer therapeutics based on antimicrobial peptides.

Abbreviations

AMP	Antimicrobial peptides
AtMP1	First antimicrobial peptide
AtMP2	Second antimicrobial peptide
<i>A. testudineus</i>	<i>Anabas testudineus</i>
ATCC	American Type Culture Collection
ATM	Ataxia-telangiectasia mutated
ATR	Ataxia-telangiectasia and Rad3 related
cDNA	Complementary deoxyribonucleic acid
CFU	Colony-forming unit
Chk1	Checkpoint 1
Chk2	Checkpoint 2
dH ₂ O	Distilled water
DMEM	Dulbecco's modified eagle medium
DNA	Deoxyribonucleic acid

¹Department of Biological Sciences and Biotechnology, Faculty of Science and Technology, Universiti Kebangsaan Malaysia, 43600 Bangi, Selangor Darul Ehsan, Malaysia. ²Department of Food Sciences, Faculty of Science and Technology, Universiti Kebangsaan Malaysia, 43600 Bangi, Selangor Darul Ehsan, Malaysia. ³Department of Earth Sciences and Environmental, Faculty of Science and Technology, Universiti Kebangsaan Malaysia, 43600 Bangi, Selangor Darul Ehsan, Malaysia. ⁴Innovative Center for Confectionery Technology (MANIS), Faculty of Science and Technology, Universiti Kebangsaan Malaysia, 43600 Bangi, Selangor Darul Ehsan, Malaysia. ⁵Faculty of Health and Life Sciences, Inti International University, Persiaran Perdana BBN Putra Nilai, 71800 Nilai, Negeri Sembilan, Malaysia. ⁶Department of Biomedical Science, Faculty of Medicine & Health Sciences, Universiti Putra Malaysia, 43400 UPM Serdang, Selangor Darul Ehsan, Malaysia. ⁷Chini Lake Research Centre, Faculty of Science and Technology, Universiti Kebangsaan Malaysia, 43600 Bangi, Selangor Darul Ehsan, Malaysia. ✉email: shazrul@ukm.edu.my

DSB	Double strand break
EDTA	Ethylenediaminetetraacetic acid
F2	Fraction 2
FACS	Fluorescence-activated cell sorting
FBS	Fetal bovine serum
gDNA	Genomic DNA
Gy	Gray, irradiation unit
HS27	Human foreskin fibroblast
LCMS	Liquid chromatography mass spectrometry
MCF7	Metastatic breast cancer (adenocarcinoma)
MDA-MB-231	Epithelial human breast cancer cell
NaCl	Sodium chloride
PBS	Phosphate buffered saline
PCR	Polymerase chain reaction
PI	Propidium iodide
SDS-Page	Sodium dodecyl sulfate polyacrylamide gel electrophoresis
UV	Ultraviolet

Breast cancer poses a crucial public health concern, which needs more molecular-level study to identify its prognosis and clinical care^{1,2}. It has become apparent in recent years that breast cancer does not constitute a single disease but rather a variety of molecularly distinct tumours that emerge from the breast's epithelial cells. Cell lines tend to be a key element in the molecular diagnosis of breast cancer, as they can be widely used in many aspects of laboratory research and particularly in cancer research as in-vitro models³. A broad range of marine animal's organisms has been identified as a source of possible therapeutic and medicinal qualities⁴⁻⁶. Fishes, algae, and sponges were reported to contain anticancer, antiproliferative, antioxidant and antimicrobial effects^{7,8}. Besides, a variety of bioactive substances have extracted from fish muscle proteins, peptides, collagen and gelatine, fish oil, and fishbone as potential bioactive compounds^{4,9}.

Antimicrobial peptides (AMPs) had garnered the attention of many researchers due to its ability to both inhibit microbes and neoplasm¹⁰⁻¹². Evidence showed that AMPs besides their antimicrobial activity they demonstrate antitumor roles, possibly in the form of a multifunctional multicellular organism host protection mechanism¹³⁻¹⁶. Hsu and co-workers have extracted two AMP from dull fish muscle by enzymatic hydrolysis with papain and protease against breast cancer human cell line MCF7¹⁷. Hydrophobic AMPs obtained from anchovy fish sources has been able to cause apoptosis in human U937 lymphoma cells by growing caspase-3 and caspase-8 activity¹⁸. Tilapia (*Oreochromis mossambicus*) hepcidin TH2-3 has been tested on multiple lines of tumour cells, which showed that human fibro sarcoma (HT1080 cell line) proliferation was inhibited¹⁹. Meanwhile, Chang and co-workers have examined an antimicrobial peptide (TH1-5) to determine antitumor activity in cancer cells, including human cervix adenocarcinoma cells (HeLa), human hepatocellular carcinoma cells (HepG2), human fibro sarcoma cells (HT1080), Cercopithecus aethiops kidney cells (COS-7), and human kidneys cells (WS-1)²⁰.

Climbing perch *Anabas testudineus* fish are common in Asia, where they are used source of food. The epidermis is characterized by a thick coat of slime containing lipids, proteins, mucopolysaccharides, and other enzymes which are essential in ensuring the preservation of moisture in the skin, thus facilitating the survival of fish at the harsh environment, especially during land movement^{21,22}. Evidence showed that proteins in bioactive crude extracted from *A. testudineus* have potential antibacterial and haemolytic activities²¹. However, the physicochemical parameters which determine some of the *A. testudineus* AMPs activities against cancer cells are still unknown, considering that the characteristics of AMPs and anticancer peptide (ACPs) are very similar^{23,24}. Due to these facts, developing research in this field is important in addressing such issues¹. Thus, this study aimed to examine the antibacterial and anticancer activities for mucus fraction extracts of *A. testudineus* fish. More importantly, we investigate the role and pathway of these fractions in inhibiting the proliferative of breast cancer cell lines. We also investigate the change in gene expression resulted from the mechanism of action of these fractions.

Materials and methods

Sample preparation. A total of 30 climbing perch with an average weight of 300 g was obtained from a local fish farm in Jelebu, Negeri Sembilan, Malaysia. The fishes were acclimatised for 7 days (in a group of three) in a 26 × 17 × 19 cm plastic aquarium at a temperature of 28 °C, at pH range between 6 and 6.5. The water used in this experiment was dechlorinated tap water. The fish were fed a commercial pelleted diet (ad libitum composed of protein, 18–50%; lipids, 10–25%; carbohydrate, 15–20%; ash, <8.5%; phosphorus, and trace amounts of vitamins, minerals, and water) for the entire period of the experiment. All experiments conducted were approved by Universiti Kebangsaan Malaysia (UKM) animal ethics committee (Ethics code: FST/2019/MOHD SHAZRUL FAZRY/25 SEPT./1034-SEPT.-2019-FEB-2020). All the methods accordance with ARRIVE guidelines.

Crude mucus collection. The Mucus of the selected *A. testudineus* was extracted as described by Ross et al.²⁵ with slight modifications. The selected fish were anaesthetised using Tricaine methane-sulfonate (MS-222). The epidermal mucus (EM) was collected from the dorsal side using a cell scraper, then transferred to a 15 ml falcon tube containing 3 ml buffer solution (pH 7.4) having 0.013 M Tris, 0.12 M NaCl, and 0.003 M KCl. The collected mucus was centrifuged at 1000×g for 10 min at 4 °C and stored at – 80 °C for further use.

Mucus purification. The frozen EM was thawed and centrifuged at 1000×g for 10 min at 4 °C to remove insoluble particles. The supernatant was collected, and once again centrifuged at 2000×g for 10 min at 4 °C. The

supernatant was collected and freeze dried (Labconco 74200-30). The lyophilised EM powder were weighted and kept in $-80\text{ }^{\circ}\text{C}$ for further use²⁵. To prepare purified EM stock solution, 0.5 g of EM powder was resuspended in 5 ml of distilled water²⁵, centrifuged at $2500\times g$ for 5 min at $4\text{ }^{\circ}\text{C}$, and used for further studies.

Mucus protein content. The protein content of EM was quantified using Bradford's (1976) technique. The purified EM stock solution (0.5 ml) was mixed with 1.5 ml of Bradford reagent. The samples were incubated at room temperature for 10 min and then the absorbance was read at 595 nm by using Shimadzu 160 UV-Vis double beam Spectrophotometer. The bovine serum albumin (BSA) was used as the standard.

Fractioning of crude mucus of *A. testudineus*. The crude mucus was fractionized as described by Yang et al.²⁶ with slight modifications. The 0.5 g purified freeze-dried mucus was resuspended in 5 ml distilled water and loaded on to Sephadex G-25 column (10 cm, 50 ml bed volume), then equilibrated with 50 ml of 0.1 M acetate buffer, pH 4.3 in the cold room using a Dynamix peristaltic pump to control the flow rate. After equilibrating 5 ml of sample is loaded onto the column, which is then washed with tris-base buffer at pH 8 to elute the sample skin mucus. Each fraction (0.5 ml) was collected in microcentrifuge tubes after concentrated by ultra-filtration using viva spin nominal molecular-mass limit of 6000 kDa. The protein concentration of the extract is determined by Bradford assay as described in "Mucus protein content". Dextran blue was used as a positive control²⁶. The fraction protein profile was detected by sodium dodecyl sulphate-polyacrylamide gel. The protein profile was run in 12% sodium dodecyl sulphate-polyacrylamide gel electrophoresis (SDS-PAGE). A mixture of 4.0 ml of 30% acrylamide, 2.6 ml of 1.5 M Tris buffer (pH 8.8), 3.2 ml of water, 100 μl of 10% SDS, 100 μl of 10% APS, and 10 μl of TEMED was mixed to make the 12% running gel. Then, a mixture of 2.6 ml of 0.5 M Tris buffer (pH 6.8), 5.86 ml of water, 1.34 ml of 30% acrylamide, 100 μl of 10% SDS, 100 μl of 10% APS, and 10 μl of TEMED were applied to prepare a 4% stacking gel. The protein was solubilized at $1\times$ volume of reducing sample buffer that was composed of 1 M Tris-HCl (pH 6.8), 50% glycerol, 10% SDS, 5% β -mercaptoethanol, water, and 1% bromophenol blue. The buffer was incubated for 5 min at $95\text{ }^{\circ}\text{C}$ and kept on ice before being loaded to the gel. The gel was applied to a Bio-Rad electrophoresis apparatus for 2 h at 30 V throughout preliminary voltage, followed by 150 V until 2 mm from the gel base. The obtained bands were observed for the Coomassie Brilliant Blue G-250 stains.

Identification of peptide sequences. Each protein sub-fractions from "Fractioning of crude mucus of *A. testudineus*" were hydrolysed by trypsin at an enzyme to the protein ratio of 1:50 at $37\text{ }^{\circ}\text{C}$ for 24 h, except the lower than 3 kDa sub-fraction. The peptides were dried by vacuum centrifuge and kept at $-80\text{ }^{\circ}\text{C}$ before conducting mass spectrometric analysis. The peptide sequence was identified by using LC-MS. In general, acetonitrile was used as the organic modifier in all separations, with concentrations ranging between 40 and 80%, by using Karpievitch and co-workers' method²⁷. The aqueous portion of the mobile phase consisted of water, ammonium acetate buffer. Flow rates were 0.4 to 0.6 ml/min for LC/MS detector and 1.0 ml/min for UV detector. All fractions were dissolved in a 50/50 mixture of water and methanol. Stock solutions, 1 mg/ml of dissolved fraction was stored in a freezer. Working solutions were made to contain 10 $\mu\text{g/ml}$ of each fraction of interest. The C_{18} separations of the fractions were conducted with the MS compatible mobile phases (aqueous acetic acid or acetate buffers with acetonitrile as the buffer) and similar flow rate conditions (0.5 ml/min vs 0.6 ml/min). UV detection was at 214 nm. This assay has been done in Liquid Chromatography-Mass Spectrometry (LCMS) Platform, LCMS Laboratory, Jeffrey Cheah School of Medicine and Health Science, Monash University Malaysia.

Bioinformatics prediction of peptides. The selected potential peptides after fractionization were then blasted against the antimicrobial peptides database: AMPfun (<http://fdlablab.csie.ncu.edu.tw/AMPfun/index.html>)²⁸; iAMP-2L (<http://www.jci-bioinfo.cn/iAMP-2L>)²⁹; and CAMP-R3 (<http://www.camp3.bicnirrh.res.in/>)³⁰. These peptides were screened for putative antimicrobial peptides by using consensus prediction. Each peptide was submitted for the prediction of two programs; ADAM (<http://bioinformatics.cs.ntou.edu.tw/ADAM/>)³¹ and ADp3 (<http://aps.unmc.edu/AP/>)³² for antimicrobial peptide prediction based on amino acid composition, conserved features, and physicochemical properties. Peptides positively predicted by both programs were considered putative antimicrobial peptides with anticancer and antimicrobial activity. These peptides were checked for toxicity and antimicrobial activity (Fig. 1).

Peptide synthesis. Two potential peptides were selected to be synthesized in-vivo. After select based on the amino acids length and predict peptide functions through in-silico database as described in "Bioinformatics prediction of peptides". We select two peptides based on molecular weight, the number of amino acids, and the net charge of these peptides as described in Table 1. These two peptides were synthesized and provided by 1st BASE Co., Ltd. (Singapore).

Disc diffusion method. The antimicrobial activity of protein fractions and synthetic peptides obtained from *A. testudineus* fish was tested against human pathogens (*Escherichia coli*, *Pseudomonas aeruginosa*, *Bacillus subtilis*, and *Bacillus cereus*). The selected microbial was spread on nutrient agar plates by using cotton bud and incubated for 24 h at $37\text{ }^{\circ}\text{C}$ ³³. The functioned discs were prepared by adding 20 μl (1000 $\mu\text{g/ml}$) of each sample (fractions and peptides) diluted in 10% ethanol on a 6 mm blank antibiotic disc. Then, the disc was placed onto the nutrient agar plate of the bacterial culture and incubated at $37\text{ }^{\circ}\text{C}$ for 24 h. A standard antibiotics disk (10 $\mu\text{g/ml}$ streptomycin) was used as the positive control while a blank disc as negative controls. After the incubation, the inhibition zones that appeared around the discs were measured to the nearest millimetre (mm).

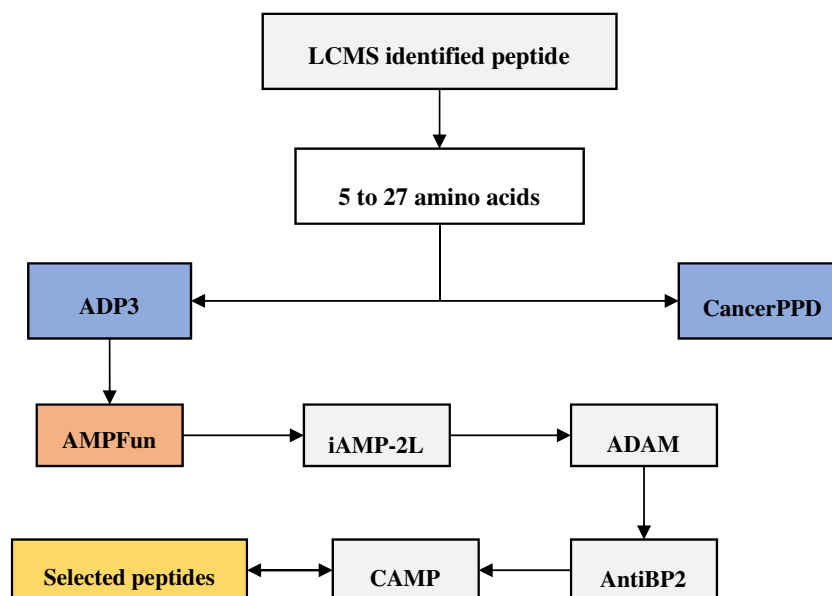


Figure 1. Workflow for bioinformatics prediction of antimicrobial peptides.

Peptide sequences	ADP3			AMPFun			iAMP-2L	ADAM	Cancer PPD	CAMP R3	AntiBP2		
	Length	Hydrophobic (%)	Net charge	Anti-cancer	Gram+	Gram-	Type	Type		No data	Type	N-terminus	C-terminus
GNLNKEMSSA PIV-GQPSIPGGPVR	24	29	1	No 0.0042	No 0.5167	No 0.4924	NON-AMPs	NON-AMPs		NAMP	Yes	Yes	Yes
GALALAPTGEVY-DIEIDL	19	47	-4	No 0.0018	No 0.3667	No 0.2242	NON-AMPs	NON-AMPs		AMP	Yes	No	No
AGVASVESSGEAF	14	42	-2	No 0.0478	No 0.4833	No 0.4778	AMPs	AMPs		NAMP	NA	NA	NA
THPPTTTTTTTTTTTTTAA PATTI	24	12	0.25	Yes 0.2816	Yes 0.5667	Yes 0.6051	AMPs	AMPs		NAMP	Yes	No	No
ACGSSTRSY-AMHIDA	15	46	0	No 0.155	No 0.35	No 0.5075	AMPs	AMPs		NAMP	No	No	Yes
TNSYPVFGAGG-GEYETI	17	23	-2	No 0.05	No 0.391	No 0.380	AMPs	AMPs		AMP	No	Yes	No
TGIATSGLATFTL-HTGSLAPAT	22	40	0.25	Yes 0.4292	Yes 0.6333	Yes 0.7233	AMPs	AMPs		NAMP	No	No	Yes

Table 1. Details on bioinformatics prediction of antimicrobial peptides from databases.

Cytotoxicity effect. *Cell lines.* Human breast cancer cell line (MCF7), human adenocarcinoma cell line (MDA-MB-231) and human skin new-born for skin fibroblast (HS27) were used in this study to determine the cytotoxicity. Cancer and normal cell lines used in this study were purchased from the American Type Culture Collection Organization (ATCC). Dulbecco's Modified Eagle Medium (DMEM) supplemented with 10% FBS and 1% penicillin. The cells were incubated at 37 °C in CO₂ 5% and humidity 85 to 95%.

Cell cytotoxicity assay. Cell cytotoxicity was performed using 3-(4, 5-dimethylthiazol-2-yl)-2, 5-diphenyltetrazolium bromide (MTT) assay³⁴. As the confluence of the cells in the flask cell reached 80%, the medium was discarded, and the cells were washed with 1× phosphate buffer saline (PBS) three times. The trypsin was added for 5–7 min, to unleash cells from the flask wall, then 5 ml of the medium was added to the flask, mixed well, transported into a new tube, and centrifuged for 5 min at 2500×g, then the supernatant was discarded. A haemocytometer chamber was used to count the cell. A 100 µl of the cell suspension with concentration of 1 × 10⁵ were seeded into 96 well plates³⁵.

After 1 day of incubation, 100 µl of extract was added into each well of 96 well plates at concentrations 1–10 µg/mL and incubated for 24 h and 48 h respectively. The cell cytotoxicity was measured by adding 10 µl of MTT reagent into the cell suspension and left for 4 h. Finally, the content of the wells was discarded, and 200 µl DMSO (100%) was added to each well and left for 15 min. The graphs are representing cell viability (%) by measuring the absorbance of optical density (590 nm) with a microplate reader.

Cell cycle analysis. The cells were seeded into 6 well plates at 1 × 10⁶ cells/well and incubated for 24 h. After incubation, the cells were treated with the fraction for 24 h, fixed in 70% ethanol, and stained with FxCycle Propidium Iodide (PI)/RNase Staining Solution (Thermo Fisher #F10797). Flowcytometry BD-FACSCanto II

(BD Bioscience, Singapore), was used to read the results. The cell cycle histogram was analysed with modified LT V.4³⁶. Three biological replicates have been used. The difference in cell cycle checkpoints was then computed in comparison to the cells without treatment.

Determination of cell apoptosis. *DNA fragmentation assay.* Lee and co-worker's method³⁷ was used to detect DNA fragmentation. The cell cultures were collected from the flask, transferred to a 15 ml tube, and centrifuged at 2800×g for 5 min. The supernatant was discarded, then 500 µl lysis buffer (pH 7.4), contain 1 ml 0.5 M Tris-HCl 3 ml 0.5 M NaCl, 0.4 ml 0.05 M EDTA, 0.03 ml Triton X-100, 0.03 ml NP40, 0.5 ml 0.05 M, 0.5 ml Sodium fluoride, 0.02 ml 0.5 M β-glycerophosphate, 0.02 ml 0.05 M Sodium orthovanadate, and 0.05 M PMSF was added, and incubated at room temperature for 10 min. The lysate cells were harvested and transferred into new tubes, then incubated at 65 °C for 5 min. After cooling at room temperature for 5 min, 700 µl chloroform-isoamyl alcohol was added, and then centrifuged at 16,000×g for 5 min. The supernatant was discarded, and the pellet was air-dried for 30 min. Then, the dried DNA was dissolved in 50 µl distilled water. A spectrophotometer Nanodrop was used to quantify the extracted DNA concentration. The DNA samples were electrophoresed on a 1.5% agarose gel containing 1 µl/100 ml SYBR-Safe DNA gel stain (Invitrogen, catalogue number: S33102).

Annexin V-FITC apoptosis. This experiment used a kit (Elabscience E-CK-A211). The cells (1×10^6 cells) were seeded in a T25 culture flask and one prepared as control (unstained, Annexin and propidium iodide only). After 48 h of incubation, the cells were trypsinized and collected by centrifugation at 1000×g for 5 min. The collected cells were washed twice with PBS and centrifuged (1000×g, 5 min, at room temperature). Each pellet ($\sim 1 \times 10^6$ cells) was resuspended in PBS (400 µl). The cells were stained using (400 µl of cells + 100 µl of incubation buffer with 2 µl of Annexin [1 mg/ml] and 2 µl of propidium iodide [1 mg/ml])³⁸. Flowcytometry BD-FACSCanto II (BD Bioscience, Singapore), was used to read the results. The cell cycle histogram was analysed with modified LT V.4³⁶. The experiments were repeated in triplicate.

RNA isolation and cDNA synthesis. Total RNA was isolated and purified from the MCF7 and MDA-MB-231 cells using the All-Prep DNA/RNA Mini Kit (QIAGEN) following the manufacturer's instructions. The cells lysate was collected and pipetted directly into a QIAshredder spin column placed in a 2 ml collection tube and centrifuged for 2 min at 16,000×g. The homogenized lysate was transferred to an All-Prep DNA spin column placed in a 2 ml collection tube, and centrifuge for 30 s at 8000×g. All-Prep DNA spin column was transferred into a new 2 ml collection tube and stored at 2 °C for later DNA purification.

For RNA elution, the cell lysate transferred to RNeasy Mine lute spin column followed by added 350 µl of 70% ethanol and mixed well by pipetting. Then, 14 µl RNase-free water was added and centrifuged for 1 min at 16,000×g to elute the RNA. The concentration and purity of the RNA were quantified using spectrophotometer (Nanodrop 1000; Thermo Fisher Scientific, Wilmington, DE, USA). The 0.5 µg of total RNA was used as a template using the RT² First Strand kit (Qiagen, Valencia, CA, USA), following the manufacturer's instructions. A spectrophotometer Nanodrop was used to quantify the extracted RNA concentration.

RT² Profiler™ PCR array. Pathway-focused gene expression profiling was performed using a 96-well human apoptosis PCR array (RT² Profiler PCR array—PAHS-apoptosis, Human PCR array, Qiagen, USA). In this array, each well contains all the components required and designed to generate single, gene-specific amplicons, testing the expression of 84 genes related to breast cancer pathways (apoptosis, metabolism, cell cycle, and DNA repair), plus 5 housekeeping genes. Each RT² Profiler PCR array plate also includes controls for data normalization, genomic DNA contamination detection, RNA sample quality and general PCR performance. The results analysis by using Gene Globe Data Analysis. Genes showed less than 1.5-fold change were neglected.

Protein-protein interaction (bioinformatics docking). Protein-protein interactions are essential to immune and cellular activities; however, there is a lack of a physiochemically-determined structure of the compounds^{39,40}. These interactions should be enrolled for a better understanding of their molecular basis. To predict the protein-peptide complexes, this study utilized various databases, including QuickDBD (<https://www.quickdatabasediagrams.com>)⁴⁰, RCSB PDB (<https://www.rcsb.org>)⁴¹, HPEPDOCK (<http://huanglab.phys.hust.edu.cn/hpepdock>)⁴², ZDOCK (<https://zdock.umassmed.edu>)³⁹, and the ligand and protein files were prepared through BIOVIA Discovery Studio Visualizer (DSV) version 20.1.0 software⁴³.

First of all, the peptides' sequence was submitted to QuickDBD to obtain the best model of the peptides' structure and select the best score model in a PDB file format. Then, the interacted protein in the RT² profiler PCR array was submitted to RCSB PDB to get the PDB file format of the protein structure and its chains. After that, the PDB files of peptides and the protein model were submitted to HPEPDOCK and ZDOCK to obtain and select the best docking model of the protein-peptide complexes based on the Z scoring. Finally, the selected protein-peptide complex model was inserted into BIOVIA DSV software to visualize the structure and obtain the protein-peptide interaction figure with different perspectives (Fig. 2).

Immunoprecipitation and pull-down assay. *Total protein extraction.* In this stage, the study used Radioimmunoprecipitation assay buffer (RIPA buffer) to lysis and extraction proteins (catalogue number: 89900) for cells' total protein extraction adapted from Zhu et al.⁴⁴. The culture media was discarded from the flask, and cells were washed twice by using 1× PBS. Subsequently, 1 ml of lysis RIPA buffer was added for 1×10^7 of cells; then, the cells were trypsinized and accumulated by using a cell scraper and kept in 1.5 ml of microcentrifuge tube. The collected cells were incubated at 4 °C for 20 min; after that, the cells were centrifuged at 13,000×g for

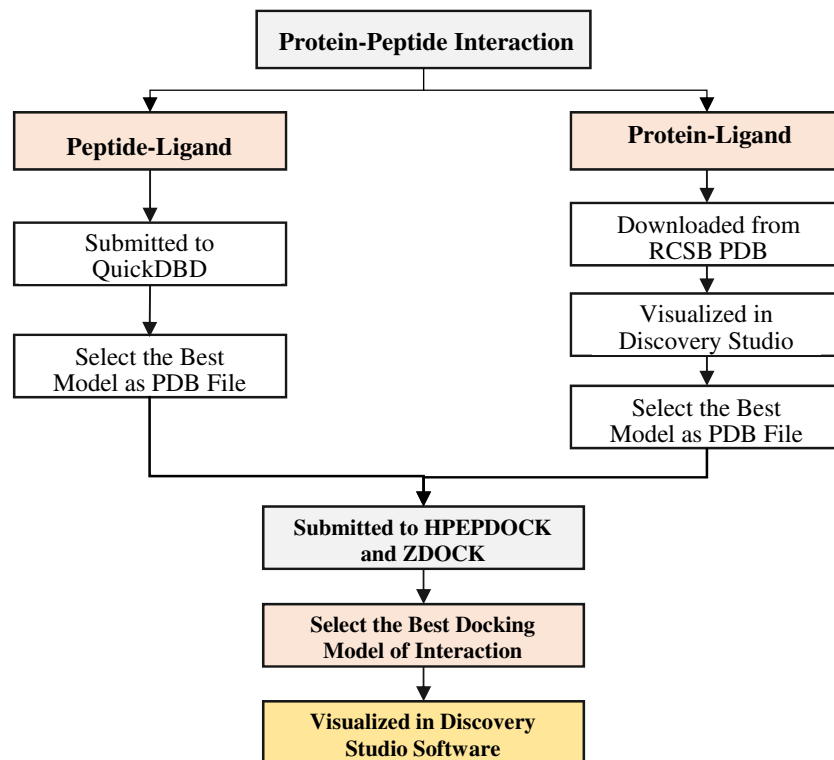


Figure 2. Workflow for protein-peptide docking interaction.

20 min at 4 °C. Finally, the supernatant consist of the soluble protein was carefully transported to a new micro-tube, and the cell pellet was discarded. Then the protein kept in – 80 °C for further study. A spectrophotometer Nanodrop was used to quantify the extracted protein concentration.

Peptide labelling. For peptide labelling, this study used Biotin Labelling Kit NH₂ (catalogue number: KA0003) by to adhering the manufacturer's guidelines instructions. 100 µl washing buffer and 200 µg selected AMPs were added in a filtration tube; then, the mixture was pipetted up and down and centrifuged at 8000×g for 10 min. Subsequently, DMSO 10 µl was added to NH₂ reactive biotin and dissolved with vortex. A reaction buffer of 100 µl with 8 µl of NH₂ reactive biotin was added to a filtration tube, mixed gently, and incubated for 10 min at 37 °C. This was followed by the addition of 100 µl of WS buffer to the tube and centrifugation at 8000×g for 10 min and discarding of the filtrate (this step was repeated twice). A 200 µl WS buffer was added to the tube and pipetted 10 times to recover the conjugate. The solution was transferred to a microtube and stored at 5 °C.

Immunoprecipitation. The extracted proteins from the cell protein extraction method (see “[Total protein extraction](#)”) were pooled with the conjugated peptides from the previous stage (see “[Peptide labelling](#)”) to link the cell protein with the peptides using Cheah and Yamada's technique⁴⁵. In this method, 200 µl of cell proteins were incubated with 20 µl of Streptavidin and kept on a rotator overnight at 4 °C to isolate biotinylated proteins from cell lysates. The beads were firstly washed with lysis buffer and transferred into a new tube and washed again with 2% SDS in 50 mM Tris HCl pH 7.4. Secondly, the biotinylated proteins were eluted from these beads by using 30 µl of 25 mM biotin for 5 min at 95 °C. After considerable wash, binding proteins were eluted by boiling in SDS sample buffer composed of 1 M Tris–HCl (pH 6.8), 50% glycerol, 10% SDS, 5% β-mercaptoethanol, and water. By using 50 mM DTT, the bait peptides with their bound proteins were removed from the beads. Thirdly, a sample buffer 4×, 80 µl was added to the beads with 200 mM Tris HCl pH 6.8, 40% glycerol, 8% SDS, 8% β-mercaptoethanol, and 0.04% bromophenol blue, and heated at 95 °C for 5 min. Subsequently, the biotinylated proteins were detected by sodium dodecyl sulphate–polyacrylamide gel. The protein profile was run in 12% sodium dodecyl sulphate–polyacrylamide gel electrophoresis (SDS-PAGE). A mixture of 4.0 ml of 30% acrylamide, 2.6 ml of 1.5 M Tris buffer (pH 8.8), 3.2 ml of water, 100 l of 10% SDS, 100 µl of 10% APS, and 10 µl of TEMED was mixed to make the 12% running gel. Then, a mixture of 2.6 ml of 0.5 M Tris buffer (pH 6.8), 5.86 ml of water, 1.34 ml of 30% acrylamide, 100 µl of 10% SDS, 100 µl of 10% APS, and 10 µl of TEMED were applied to prepare a 4% stacking gel. The protein was solubilized at 1× volume of reducing sample buffer that was composed of 1 M Tris–HCl (pH 6.8), 50% glycerol, 10% SDS, 5% β-mercaptoethanol, water, and 1% bromophenol blue. The buffer was incubated for 5 min at 95 °C and kept on ice before being loaded to the gel. The gel was applied to a Bio-Rad electrophoresis apparatus for 2 h at 30 V throughout preliminary voltage, followed by 150 V until 2 mm from the gel base. The obtained bands were observed for the Coomassie Brilliant Blue

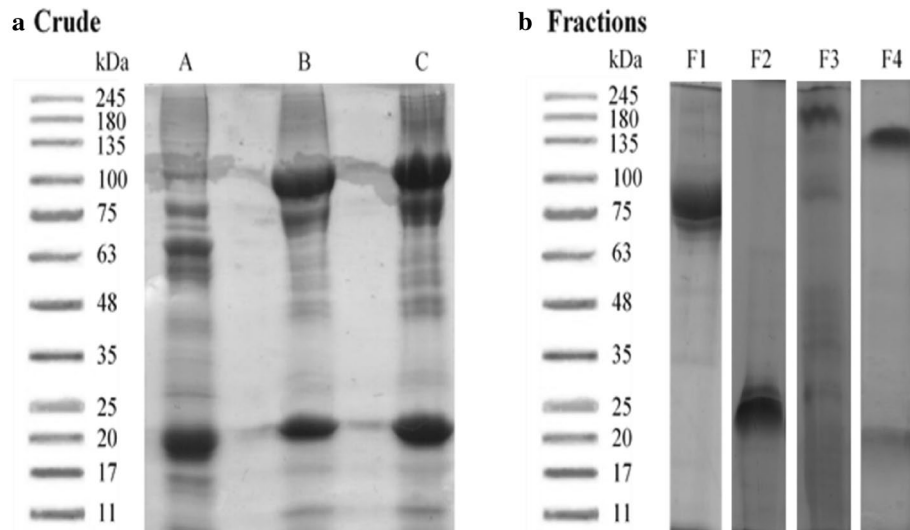


Figure 3. Protein profile for crude and fraction by 12% SDS PAGE from Sephadex G-25. **(a)** Crude mucus (AA) represents 1st replicate, (AB) represents 2nd replicate, (AC) represents 3rd replicate. **(b)** Protein fractions (F1) represents 1st fraction, (F2) represents 2nd fraction, (F3) represents 3rd fraction, (F4) represents 4th fraction. The figures are combination of different gels blot picture, and the original picture are shown in (Supplementary Figs. S1, S2, S3, S4, S5).

G-250 stains. were run on the SDS page to check the protein profile and then run with LC-MS-MS to identify the protein sequence.

Statistical analysis. All data were expressed as the mean \pm standard deviation (SD) of the values obtained from at least three replicates. A Statistical Package for the Social Sciences Program (SPSS) version 23 was used to conduct one-way analysis of variance (ANOVA), where the p -value < 0.05 was considered to be statistically significant.

Ethical approval. All authors declared that all methods and protocols were carried out in accordance with relevant guidelines and regulations. All experiments conducted were approved by Universiti Kebangsaan Malaysia (UKM) animal ethics committee (Ethics code: FST/2019/MOHD SHAZRUL FAZRY/25 SEPT./1034-SEPT.-2019-FEB-2020).

Results

Mucus collection and preparation. The epidermal mucus obtained from *A. testudineus* was scrapped to yield the mucus sample. The crude mucus content in the epidermal mucus of all selected healthy *A. testudineus* fish was 31.03 ± 0.21 mg/ml. Crude mucus that was obtained from the epidermal layer of *A. testudineus* was found to contain most of the basic biochemical components like proteins, carbohydrates, and lipids.

SDS-PAGE protein fraction profile. The protein profiles of the crude mucus protein samples of *A. testudineus* on SDS-PAGE gel showed proteins ranging from 245 kDa to less than 11 kDa (Fig. 3a). The crude mucus fractionated using Sephadex G-25 column. The protein fractions were collected, and the concentration of fraction measured using UV spectrometer at 280 nm³⁵. The total protein content of the homogenate, dialyzed fractions were found to be 112, 138, 89, and 58 mg/ml, respectively. The protein profile for the fractions were analysed by 12% SDS-PAGE, which revealed a distinct protein of molecular weight ranging from 11 to 135 kDa (Fig. 3b). The molecular weight of fractions 1, 2, 3 and 4 were 75, 25, 80, and 135 kDa, respectively.

Antimicrobial activity of protein fraction. The cytotoxicity and antimicrobial effect of the protein fractions of *A. testudineus* were evaluated in-vitro to assess their activity. Among these fractions, only F2 show significant antimicrobial activity. This fraction showed higher antibacterial activities against the human pathogen (*E. coli*, *P. aeruginosa*, *B. subtilis*, and *B. cereus*) compared to the streptomycin as a control. The inhibition zones against *E. coli*, *P. aeruginosa*, *B. cereus*, and *B. subtilis* were 9.6 ± 0.12 , 8.8 ± 0.20 , 4.4 ± 0.62 and 4.1 ± 0.15 mm respectively (Fig. 4). These values are significantly higher compared to streptomycin (control) against *E. coli* (3.8 ± 0.18 mm) and *P. aeruginosa* (3.6 ± 0.18 mm), but no significant different for *B. cereus* and *B. subtilis*. The correlation analysis using the bivariate analysis at 95% confidence level showed significant results ($p < 0.01$) between EM and streptomycin (control) of *E. coli* and *P. aeruginosa* pathogens.

Cytotoxic effect of protein fraction. The cytotoxicity effect of F2 was assessed using MTT assay against human breast cancer cell line (MCF7), human adenocarcinoma cell line (MDA-MB-231), and normal cell,

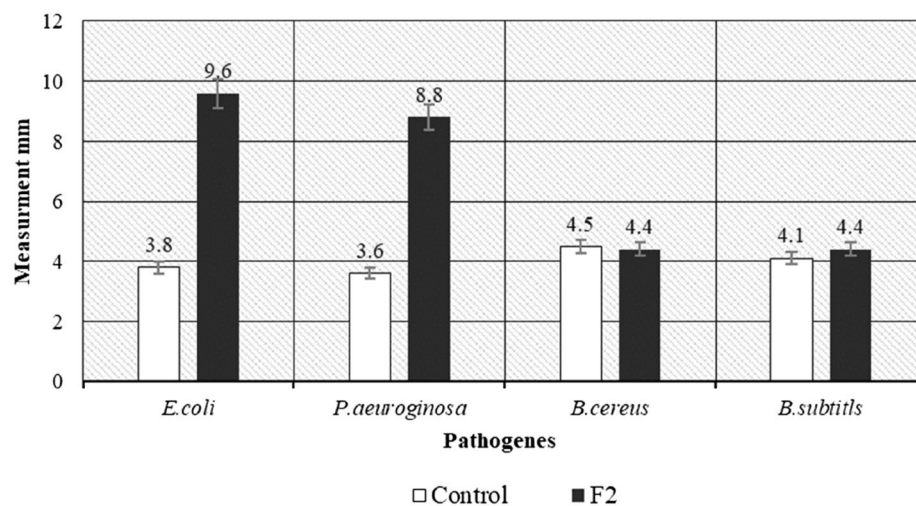


Figure 4. Antibacterial activity of F2 using disk diffusion method.

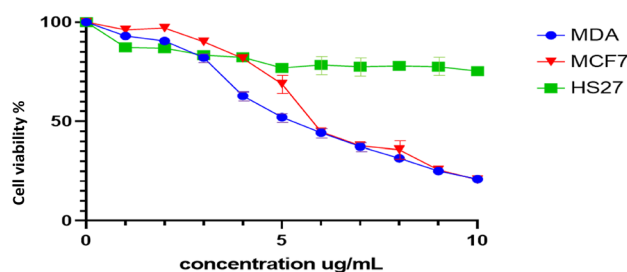


Figure 5. Cytotoxicity activity of F2 using MTT assay.

human new-born for skin fibroblast (HS27). These cells were treated with F2 at different concentration 1–10 µg/ml for 24 h and 48 h (Fig. 5). This treatment showed that the percentage of cell viability gradually decreased as F2 concentration increased. The IC_{50} value of those cells (MCF7, and MDA-MB-231) treated for 48 h with F2 were 5.02 ± 0.4 µg/ml and 4.97 ± 0.25 µg/ml respectively. This treatment shows no significant effect on normal cells (new-born skin fibroblast). The cytotoxicity results showed that F2 has cytotoxicity effects against cancer cells while did not show any effects against normal (healthy) human cells.

Cell cycle profile. Fluorescence-activated cell sorting (FACS) is a specialized type of flow cytometry in which utilizes light to count and profile cells in a heterogeneous fluid mixture. In this study, the cell cycle treated with F2 were observed for 48 h. The cancer cell cycle of MCF7 and MDA-MB-231 was observed at four-time points (6 h, 12 h, 24 h, and 48 h) and compared with the normal cell lines HS27 at the same conditions (Fig. 6). Compared to the untreated, F2 arrested the growth of MCF7 and MDA-MB-231 cells at the G0/1 phase. F2 did not show any effects on the cell cycle of HS27. In this study, HS27 has been used to study and evaluate the effects of F2 on normal cells. F2 arrested the growth of MCF7 and MDA-MB-231 cells at the G0/1 phase but not HS27. The arrest of cells growth at the G0/1 phase is very important as it will block the cancer cells from entering the S-phase resulting in DNA damage^{19,34}.

DNA fragmentation assay. To detect apoptosis, this study employed DNA fragmentation assay by using 1.2% agarose gel electrophoresis on the DNA extracted from MCF7, MDA-MB-231, and HS27 cells that was treated with 5 µg/ml F2 for 48 h incubation. It was found that the DNA obtained from control samples was intact and represented as a prominent single band on the gel. On the contrary, the electrophoretic DNA obtained from cell lines treated with F2 has a few fragments. Results showed that breast cancer (MDA-MB-231 and MCF7) cell lines treated with 5 µg/ml of the F2 samples showed higher fragmentation than HS27 as control (Fig. 7).

AMPs selection and synthesis. This study found that F2 was able to reduce cell viability. These results led to the hypothesis that peptides or proteins within the F2 could have different cytotoxic mechanisms against the cells. Modification of these peptides or proteins could enhance specificity to the MCF-7 and MDA-MB-231 cells. Thus, F2 was selected for peptidomics analysis. This fraction was then further separated by SDS-Page, digested, and directly subjected to the LC-MS/MS analysis.

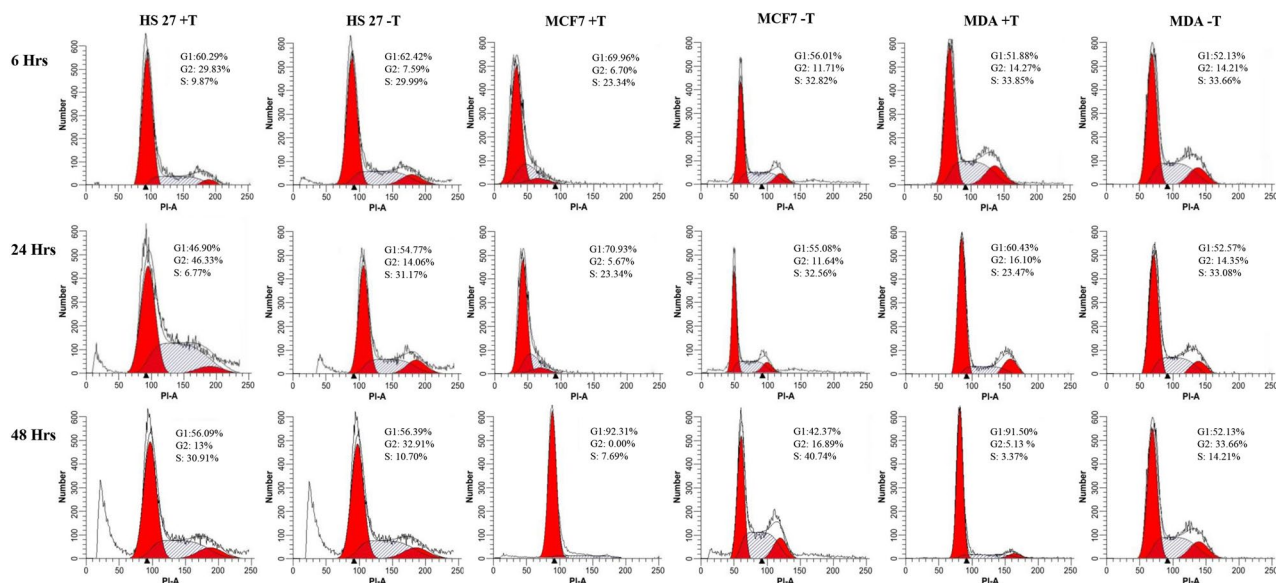


Figure 6. Cell cycle profile for cells after treatment with F2. (+ T) treated sample, (- T) untreated sample.

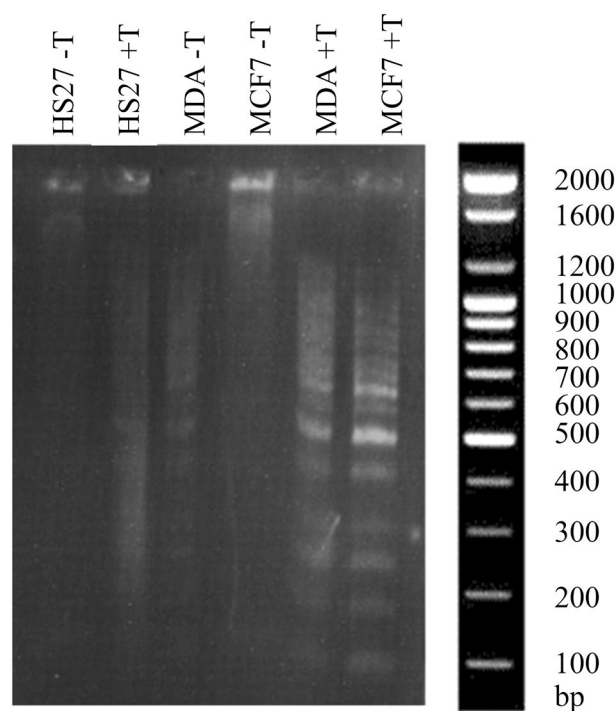


Figure 7. DNA fragmentation assay for cells after treatment with F2. (HS27-T) Represented non-treated HS27, (HS27 + T) Represented treated HS27, (MDA-T) Represented non-treated MDA-MB-231, (MDA + T) Represented treated MDA-MB-231, (MCF7-T) Represented non-treated MCF7, (MCF7 + T) Represented treated MCF7.

Four bioinformatics programs including ADP3, AMPfun, ADAM and AntiBP2 were used to predict putative AMPs from the mass spectrometric-detected peptides. Seven putative AMPs were predicted from F2 which having positive prediction scores. Most of the predicted putative AMPs have a molecular weight less than 10 kDa with length ranging from 17 to 25 amino acids. Analysis of physicochemical properties of these 7 putative AMPs by ADP3 showed a higher average score of hydrophobicity from 47 to 12% and net charge from - 2 to + 2, as shown in Table 1. Then the physicochemically properties and N-terminus, C-terminus, and NC-terminus for those

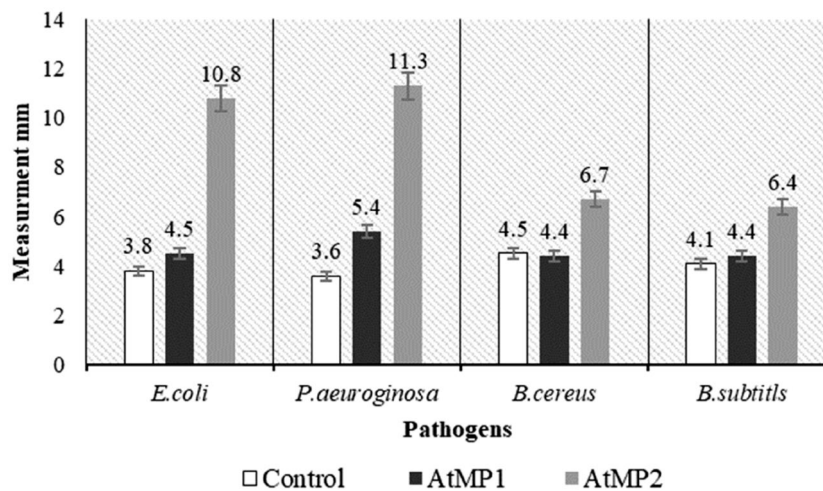


Figure 8. Antibacterial activity of peptides using disk diffusion method. The data were expressed as the mean \pm standard deviation (error bar) for three replicates.

peptides were referenced in ADAM and AntiBP2 data bases. Two peptides were identified by AMPfun having good properties to function as antibacterial and anticancer (Table 1). Both have sequence “THPPTTTTTTTTTTTTTTAAAPATTT”, and “TGIATSLGATFTLHTGSLAPAT”. These two sequences were used for production of synthetic AMP and coded as AtMP1 and AtMP2 respectively.

Antimicrobial activity of AMPs. The disc diffusion method was used to test the antimicrobial activity of AtMP1 and AtMP2 against the human pathogens (*E. coli*, *P. aeruginosa*, *B. subtilis*, and *B. cereus*) while compared to streptomycin as control. The diameter of inhibition zone formed were presented in Fig. 8. It was found AtMP2 significantly have higher antimicrobial activity compared to AtMP1 and commercial antibiotic, streptomycin. The correlation analysis using the bivariate analysis at 95% confidence level showed significant results ($p < 0.01$) between AtMP2, AtMP1 and the control. The antimicrobial activity of AtMP2 is even higher compared to their parent fraction, F2 (Fig. 4).

Cytotoxic effect of AMPs. Peptide cytotoxicity effect against the MCF-7, MDA-MB-231 and HS27 were analysed by MTT assay for concentration range from 1 to 10 $\mu\text{g/ml}$. It was found increased in concentration of peptides significantly reduced the viability of all cells. However, both peptides didn't show a significant effect against HS27 cell-line (Fig. 9). The IC_{50} of the AtMP1 against MCF7 and MDA-MB-231 were 8.25 ± 0.14 and 9.35 ± 0.25 $\mu\text{g/ml}$ respectively. AtMP2 show lower IC_{50} value which were 5.89 ± 0.14 and 6.97 ± 0.24 $\mu\text{g/ml}$ against MCF7 and MDA-MB-231 respectively.

Annexin V-FITC apoptosis assay. To detect the apoptosis of AtMP1 and AtMP2 in MDA-MB-231 and MCF7 cell-lines, Annexin V-FITC method was applied. This study used untreated breast cancer cell lines MDA-MB-231 and MCF-7 as a control to compare with the treated cell lines to check the effect of AtMP1 and AtMP2 on breast cancer cell lines. Dot-plot graphs Fig. 10, the lower right quadrant refers to early phase apoptotic cells, the upper right quadrant refers to late phase apoptosis, the upper left quadrant refers to necrotic cells, and the lower left quadrant refers to viable cells. These results indicated that at the early apoptosis stage, the mitochondrial membrane was disturbed, and the phosphatidylserine appeared on the cell surface, which linked to Annexin V. This event is considered as one of the early apoptosis markers. Meanwhile, the nuclear membrane was lysed at the late-stage apoptosis, and the stain entered the nucleus. AtMP1 and AtMP2 showed as effective molecules that act against cancer cells either via the membranolytic pathway or by rupturing the mitochondrial membrane. As shown in Fig. 10 the early apoptotic cell populations of MCF-7 for the AtMP1 and AtMP2 at 48 h was 24.94 ± 0.53 and 26.67 ± 0.43 , and the late apoptotic cells of MCF7 were 26.98 ± 0.54 and 24.98 ± 0.56 , respectively. Untreated MCF-7 cells didn't show any apoptosis level compared to treated cells. For MDA-MB-231 early apoptotic cell populations for the AtMP1 and AtMP2 at 48 h was 25.78 ± 0.26 and 26.92 ± 0.12 , and the late apoptotic was 29.32 ± 0.31 and 28.87 ± 0.15 , respectively. Untreated MDA-MB-231 cells didn't show any apoptosis level compared to treated cells.

Gene expression profiler RT² PCR array. In order to detect the apoptosis pathway of the used cancer cells and the responsible gene regulating the apoptosis induced by the experimental treatments, the human apoptosis cancer RT² Profiler PCR Array (PAHS-012ZA) was used. This test included 84 essential gene-regulated human apoptosis. These genes relate to a specific pathway, which contains proteins (genes) that can contribute to one or more processes, including cell cycle monitoring, angiogenesis, and apoptosis. The details on fold change are summarised in Figs. 11 and 12.

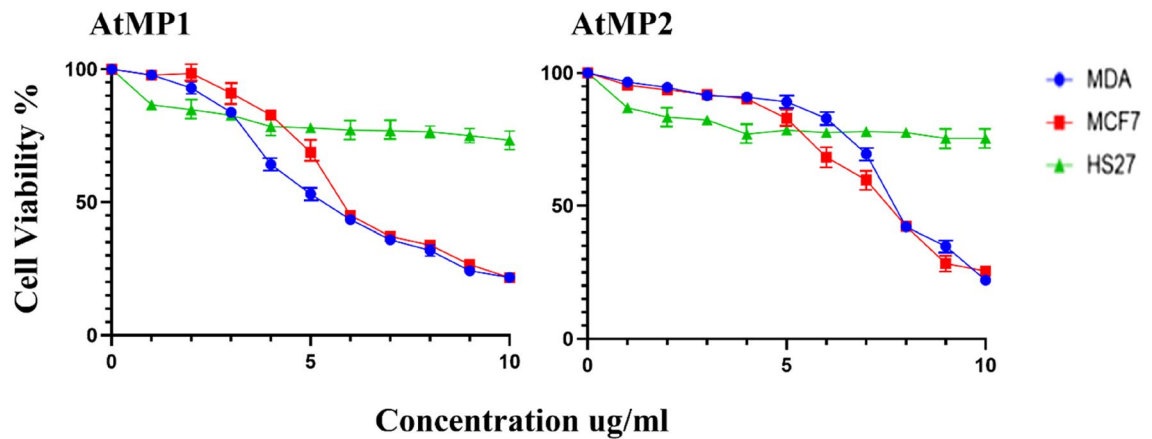


Figure 9. Cytotoxicity effect of synthesis AtMP1 and AtMP2 on cancer MDA-MB-231 and MCF7 cell line and HS27 normal cell lines. The cytotoxicity calculated and the results show the treatment was cytotoxic cancer cell line after 48 h. However, the treatment didn't show effects against normal cell line (HS27). The graphs are representing cell viability (%) by measuring the absorbance of optical density (590 nm) with a microplate reader. Data are the mean \pm SD of triplicate determinations. (Left) AtMP2. (Right) AtMP1.

In this test, many genes were observed to be upregulated or downregulated. However, these genes showed less than 1.5-fold change; therefore, it was neglected. The AtMP1 significantly upregulated the expression of four genes in the MCF7 cancer cell, including BAX, caspase-3, caspase-7, and p53, and downregulated the expression of BCL-2. For the MDA-MB-231 cancer cells, the AtMP1 enhanced the five gene expressions, including BAX, caspase-3, caspase-7, caspase-9, and p53, and diminished the expression of the BCL-2 gene. When the AtMP2 was used to treat MCF7 cancer cells, three genes were upregulated, including BAX, caspase-7, and p53, and the BCL-2 gene was downregulated (> sixfold). However, the cancer cell MCF7 treated with the AtMP1 and AtMP2 did not show any significant regulation on caspase-3, yet MCF7 led to apoptosis induction (this might be due to the activation of caspase-7).

In the MDA-MB-231 cancer cell, the AtMP2 significantly upregulated the five genes' expression (BAX, caspase-7, caspase-8, caspase-9, and p53), and diminished the BCL-2 gene. These results showed that the AtMP1 and AtMP2 could enhance the downregulation of the anti-apoptotic BCL-2 gene. Furthermore, they promoted the upregulation of pro-apoptotic genes, such as BAX; tumor suppressor genes, such as p53; and the executioner caspase family, such as caspase-3, caspase-7, caspase-8, and caspase-9, simultaneously.

Bioinformatic prediction of protein-peptide docking. After gene expression identification, this study aimed to specify the structure of the selected two peptides, the peptides' binding site and the interacted seven genes, and the interaction model. A set of five databases and software was used, including QuickDBD⁴⁰, RCSB PDB⁴¹, HPEPDOCK⁴², ZDOCK³⁹, and the ligand and protein files were prepared through BIOVIA DSV software⁴³ to detect the blind docking method of peptides to proteins. The sequence of the two selected peptides (Table 1) was submitted to QuickDBD using the Fasta format⁴⁰. The QuickDBD showed 10 models for each peptide structure. Among these models, the top-score models were selected based on the Z-score (-239.700 for the AtMP1 and -173.695 for the AtMP2 as shown in Fig. 13). The RCSB PDB protein data bank (was utilised to detect the sequence length, chain, and active site of the interacted proteins⁴¹).

After that, the model of each peptide was submitted sequentially with each protein to the HPEPDOCK database⁴², which led to identifying each peptide's binding site with the proteins. HPEPDOCK also aided in identifying the type of binding bonds and the interaction model between the peptide and proteins (peptide-protein docking) (Fig. 14).

Figure 14 indicates that the AtMP2 can be linked to BAX (THr22-Glu123, THr1-Tyr204, Glu3-Phe256, His13-Arg207, Pro20-Asn208, Ala9-Trp214/Phe247/Glu246, Lys4-His257/Glu248/Ser249) and caspase-3 (Ile3-Phe252, Ser6-Ser209, Leu8-Arg207, Ala9-Trp206, THr10-Ser205/Cys163, Phe11-His121, THr12-Gly122/Glu123, His14-Pro133/Glu123, THr22-Cys138/Lys137/Asn141/Arg147/Arg144). The AtMP2 interacted with caspase-7 (Leu8-His121/Tyr204, Phe11-Lys256/Ser251, His14-Asp253/Ser251, Gly16-Ser209) and caspase-8 (THr1-Glu115, Gly7-Tyr116, Phe11-Gly117/Tyr29/Arg33, His14-Arg33, Gly16-Tyr175, Leu18-Asp172, Ala19-Arg300).

Then, the AtMP2 was linked to caspase-9 (Ala4-Pro198, THr5-Glu180, Ala9-Leu179, Phe11-Asp296, His14-Ser247/Val297/Ser293/Asp296, Ala21-Trp305, THr22-Trp305), p53 (THr1-Mel330/Trp62/Asp65, His13-Trp62/Lys15/Trp230/Asp14, Pro20-Phe156/Tyr155/Trp230/Asn12/Asp14/Lys15, Lys17-Glu38, Ala4-Asp55/Lys1, Ala19-Lys1). In addition, the AtMP2 was inserted into BCL-2 (Ala4-Pro189, THr5-Glu180, Ala9-Leu179, THr10-Glu292, Phe11-Asp296, His14-Ser247, Val297, Asp296, Ser293, THr22-Trp305).

For reliability, the ZDOCK database³⁹ was utilised to confirm the interaction model of each peptide that interacted with the proteins. Finally, the predicted models of the peptide-protein docking were visualised and modified using BIOVIA DSV software⁴³ as shown in Fig. 15. These databases provided useful tools for investigating peptide-protein docking, modelling, and reconstruction. Notably, the findings obtained from these databases proved the validity of gene expression results, in which the two peptides extracted from *A. testudineus* could

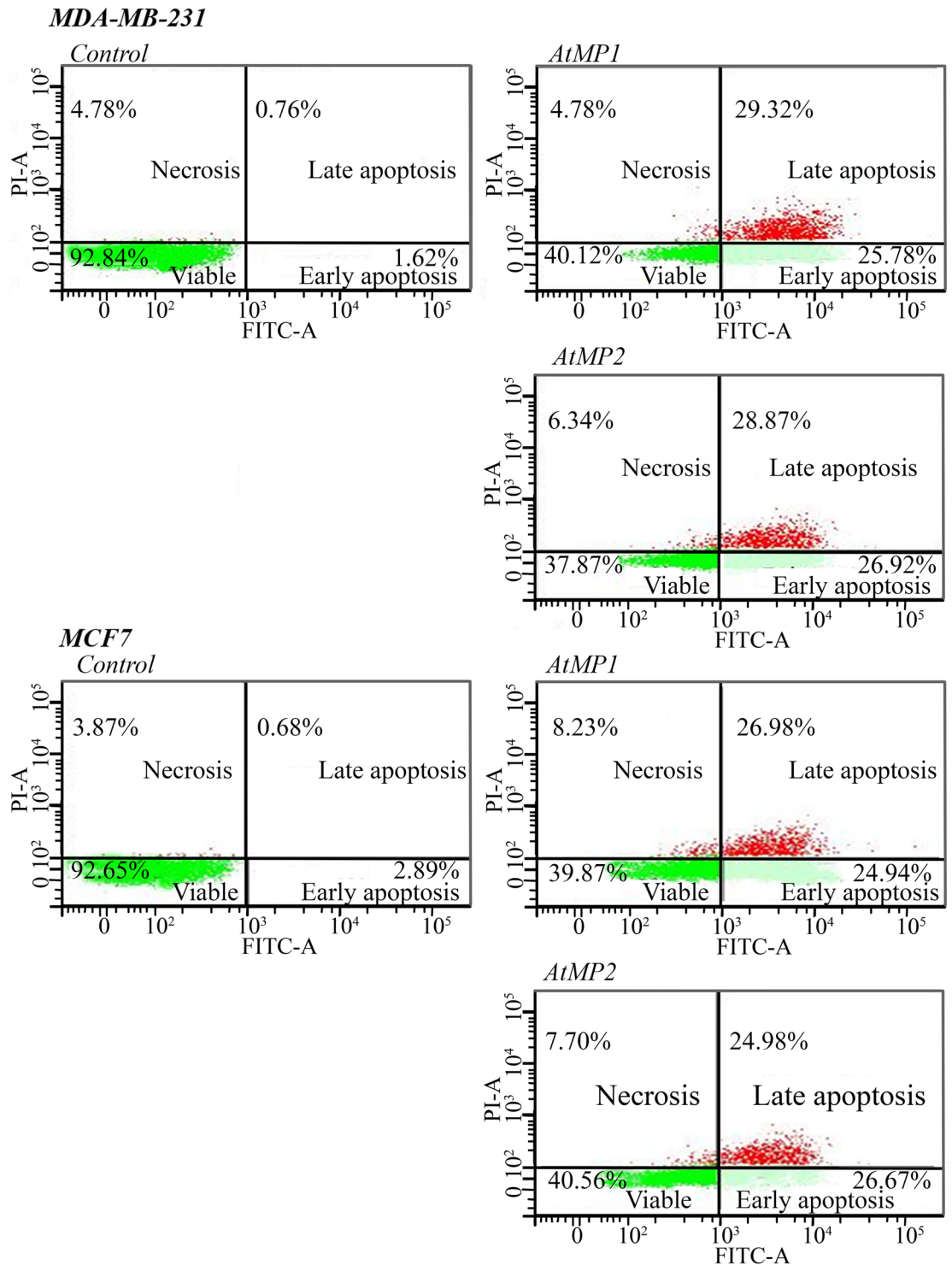


Figure 10. Apoptosis detection results by Annexin V FITC-A assay.

modulate the expression of the genes (BAX, caspase-3, caspase-7, caspase-8, caspase-9, p53, and BCL-2). All the data bases websites links and date of access were provided in Supplementary Table S5.

Immunoprecipitation pull-down assay. Immunoprecipitation was carried out of 1.5 mg total cell lysates extracted from MCF7 and MDA-MB-231 cells using agarose beads to study the protein-peptide interaction network. The cell lysates (the total, mitochondrial, membrane, and nucleus) of non-treated cell lines were extracted and run in SDS-PAGE along with marker size ranging from 11 to 245 kDa. Results show the present of the high and low molecular weight (MW) bands in the range of 11–245 kDa (Fig. 16A). Then, both breast cancer cell lines (MCF7 and MDA-MB-231) were treated with biotinylated peptides, AtMP1 and AtMP2, and incubated for 48 h. Both peptides treated cell lysates were extracted and precleared with the same material used in immunoprecipi-

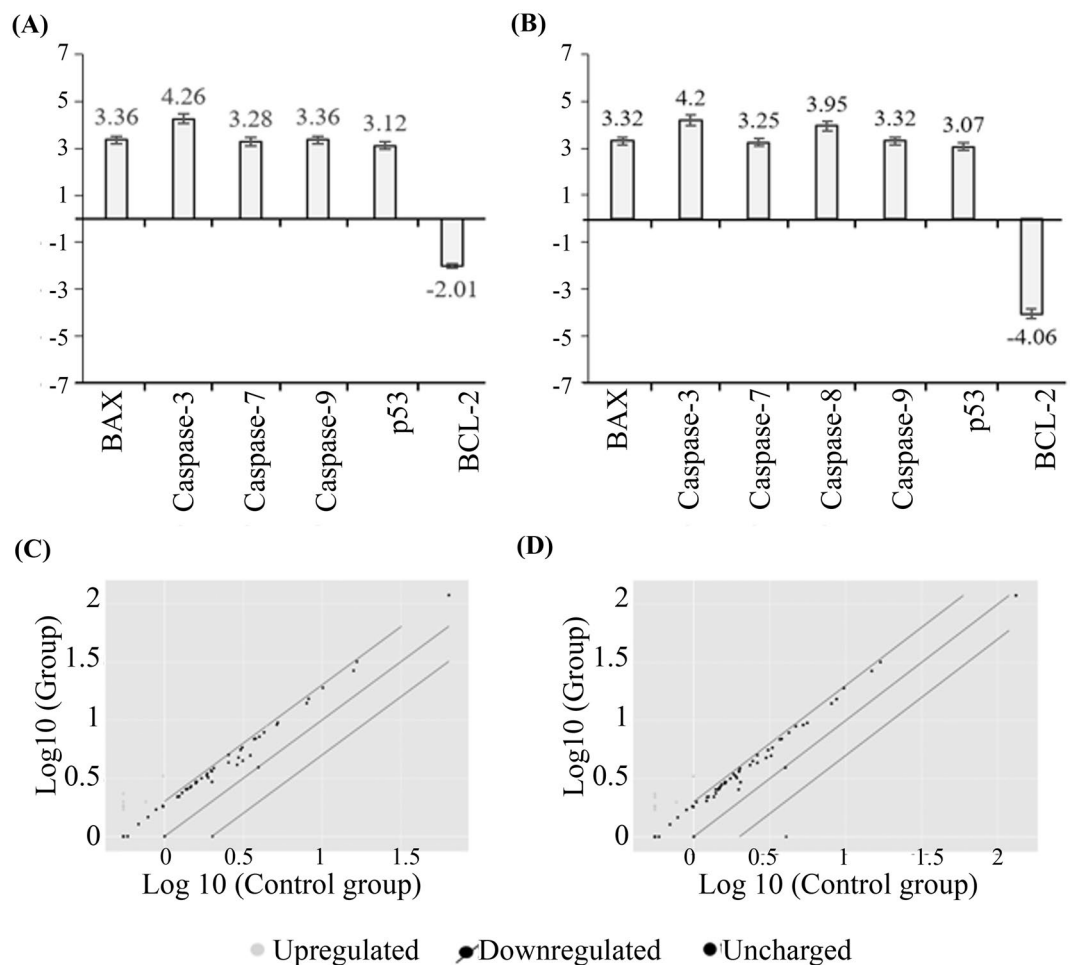


Figure 11. RT² Profiler PCR Array (PAHS-012ZA) for MDA-MB-231 cell lines. (A) The fold change values for cancer cells treated with the AtMP1, (B) fold change values for cancer cells treated with the AtMP2. (C) The Scatter Plot compares every gene's normalized expression on the PCR Array for cancer cells treated with the AtMP1, (D) the Scatter Plot compares the normalized expression of every gene on the PCR Array for cancer cells treated with the AtMP2. The results analysis by using Gene Globe Data Analysis. Genes showed less than 1.5-fold change were neglected. The full list of genes was mentioned in supplementary figures file (Supplementary Tables S1, S2).

tation to reduce nonspecific binding proteins and run in SDS-PAGE along with same marker size (11–245 kDa) (Fig. 16B).

The specific possible bands of apoptosis related proteins; caspase-3 (20 kDa), caspase-7 (21 kDa), caspase-8 (25 kDa), caspase-9 (50 kDa), p53 (55 kDa), and Bax (40 kDa) (Fig. 16B), were excised based on their MW range, digested, and analyzed by Nano liquid chromatography-tandem mass spectrometry (Gel-Nano LC-MS/MS) as presented in Supplementary Table S6.

Subsequently, the LC-MS peak list files were used to query NCBI, Swiss-Port, and Mascot 2.0 databases were applied for protein detection and identification. Only significant hits as defined by Mascot probability analysis were considered. Peptide hits were accepted when the ion score exceeded a value of 20. Protein hits required at least one peptide hit exceeding a peptide score of 20. Protein identifications were accepted with a statistically significant Mascot protein search score \geq of 20 which corresponds to an error probability of $P < 0.05$. The apoptotic proteins identification with the adequate score was selected. The specific apoptosis proteins were identified via using LC-MS and NCBI, Swiss-Port, and Mascot 2.0 databases.

Overall, the combined LC-MS data resulted in the identification of 55 distinct protein species. A total of 55 proteins were identified and arranged in descending order based on their Mascot protein search score^{27,55} (Supplementary Table S6). Seven apoptotic proteins (p53, BCL-2, BAX, Caspase-3, Caspase-7, Caspase-8, Caspase-9) were found in the list of 55 proteins (Fig. 16C).

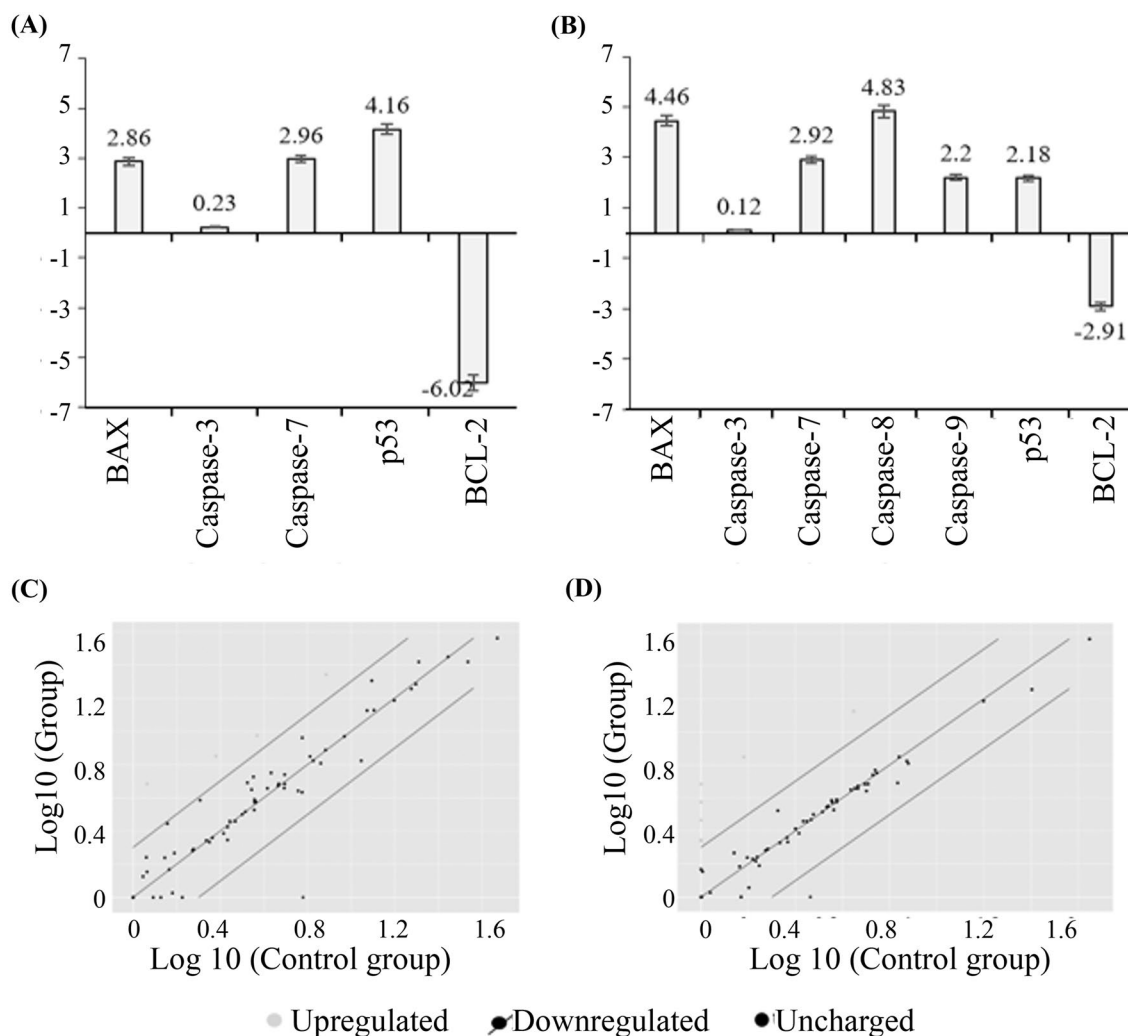


Figure 12. RT² Profiler PCR Array (PAHS-012ZA) for MCF7 cell lines. (A) the fold change values for cancer cells treated with the AtMP1, (B) fold change values for cancer cells treated with the AtMP2. (C) The Scatter Plot compares every gene's normalized expression on the PCR Array for cancer cells treated with the AtMP1, (D) the Scatter Plot compares the normalized expression of every gene on the PCR Array for cancer cells treated with the AtMP2. The results analysis by using Gene Globe Data Analysis Centre. Genes showed less than 1.5-fold change were neglected. The full list of genes was mentioned in supplementary figures file (Supplementary Tables S3, S4).

Discussion and conclusion

As far as we are aware, the present study is the first study to examine the effect of *A. testudineus* fish skin mucus on breast cancer and normal cell line. Therefore, the current study examined the effect and role of the crude and four fractions of *A. testudineus* mucus on breast cancer cell line namely MCF7 and MDA-MB-231 in comparison to human skin fibroblast (HS27) by using the MTT assay. Disc diffusion method also used to examine the antimicrobial effect of crude and four fractions of *A. testudineus* mucus against four human pathogens. Consistent with this goal, the current study found that the F2 of *A. testudineus* skin mucus inhibited the proliferative of breast cancer cell line MCF7 and MDA-MB-231 through inducing cell apoptosis. Therefore, the F2 blasted against a database of antimicrobial peptides to screen its antimicrobial and anticancer properties. This proved that the F2 contained seven antimicrobial peptides, two of them have both antimicrobial and anticancer possible activity; the AtMP1 sequence was THPPTTTTTTTTTTTAATTT, and the AtMP2 sequence was TGIATSGLATFTLHTGSLAPAT. The IC₅₀ of the AtMP1 against MCF7 and MDA-MB-231 were 8.25 ± 0.14 and 9.35 ± 0.25 $\mu\text{g/ml}$, and the IC₅₀ of the AtMP2 against MCF7 and MDA-MB-231 were 5.89 ± 0.14 and 6.97 ± 0.24 $\mu\text{g/ml}$. Also, the inhibition zone of the pathogens (*E. coli*, *P. aeruginosa*, *B. cereus*, and *B. subtilis*) treated with the AtMP1 was 4.5 ± 0.11 , 5.4 ± 0.24 , 4.4 ± 0.18 , and 4.4 ± 0.12 mm, respectively. The inhibition zone of the mentioned pathogens treated with the AtMP2 was 10.8 ± 0.24 , 11.3 ± 0.23 , 6.7 ± 0.17 , and 6.4 ± 0.21 mm, respectively (Fig. 8). From this result this study found that the AtMP2 should better activity compared to AtMP1.

The current result is consistent to the findings reported by E-kobon and co-workers who found the cytotoxicity of the crude *A. fulica* mucus against the breast cancer cell line, MCF7^{46,47}. Chen et al. also found that antimicrobial peptide TH2-3 extracted from tilapia skin mucus has an effect against human fibro sarcoma cells

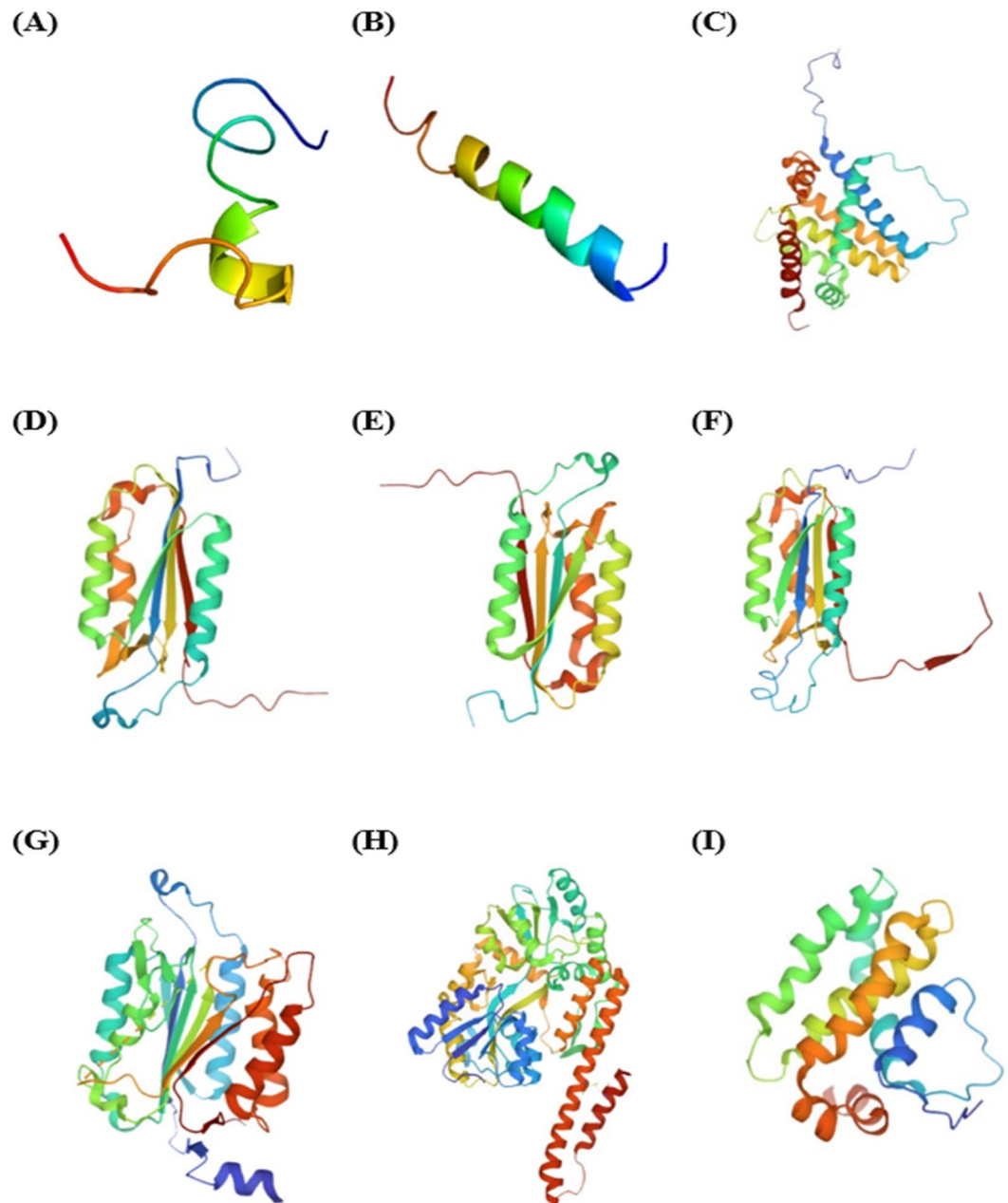


Figure 13. 3D model structure for peptides and proteins by using QuickDBD. (A) AtMP1, (B) AtMP2, (C) BAX, (D) caspase-3, (E) caspase-7, (F) caspase-8, (G) caspase-9, (H) p53, and (I) BCL-2.

(HT1080)^{19,38}. Previous studies also suggested that the fish mucus are rich sources of antimicrobial peptides, where these peptides have a significant effect as antibacterial, antifungal, and even antiproliferative^{19,48,49}. In addition, E-kobon and co-workers found that *A. fulica* mucus affected normal Vero cells. Importantly, the two peptides separated in the current study has no significant effect on the normal human skin fibroblast⁴⁶.

Additionally, the current study applied Annexin V-FITC apoptosis assay to detect the apoptosis of MDA-MB-231 and MCF7 cell-lines treated with AtMP1 and AtMP2. Both AMPs showed the capability to induce the apoptotic cancer cell death in the early and late phase at 48 h. This result is consistent with an empirical result reported by Kuo et al.⁴⁸, who confirmed that antimicrobial peptide (MSP-4) significantly induced apoptosis in osteosarcoma MG63 cells, through an intrinsic pathway and an extrinsic pathway. The prior evidence also investigated the effects of cancer agent on cell growth and apoptosis-related gene expression in breast cancer cells^{50–52}. The current study, therefore, determines the changes in gene expression of MCF-7 and MDA-MB-231 cells treated with the AtMP1 and AtMP2 by using the human apoptosis RT² Profiler PCR Array. The gene expression analysis of the current study confirmed that the AtMP1 and AtMP2 significantly increased the expression of the 5 genes of MDA-MB-231 cell, including BAX, Caspase3, Caspase7, Caspase9, and tumour suppressors TP53. BAX considered as a proapoptotic gene. In MCF7 cell, the AtMP1 and AtMP2 didn't show a significant

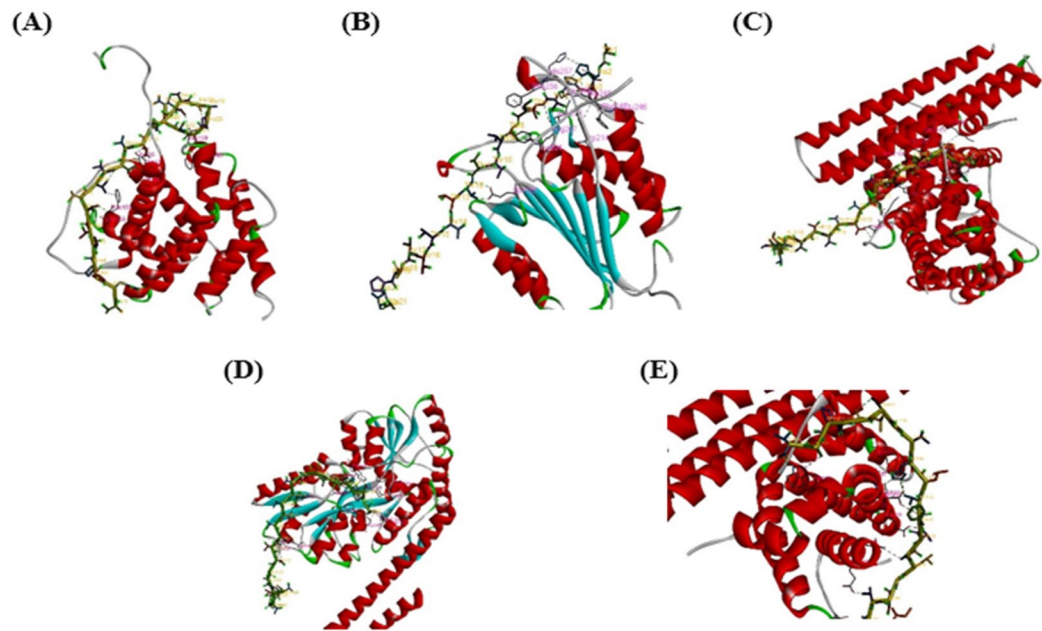
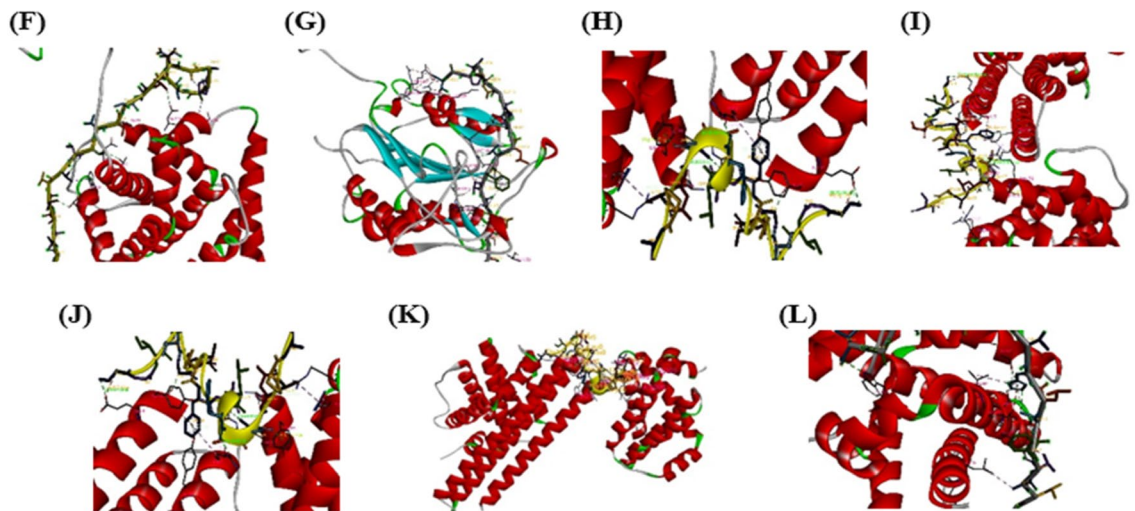
Peptide 1**Peptide 2**

Figure 14. Peptide-protein docking 3D model by using HPEDOCK. (A) AtMP1-BAX docking model, (B) AtMP1-caspase-3 docking model, (C) AtMP1-caspase-9 docking model, (D) AtMP1-p53 docking model, (E) AtMP1-BCL2 docking model, (F) AtMP2-BAX docking model, (G) AtMP2-caspase-3 docking model, (H) AtMP2-caspase-7 docking model, (I) AtMP2-caspase-8 docking model, (J) AtMP2-caspase-9 docking model, (K) AtMP2-p53 docking model, (L) AtMP2-BCL2 docking model. The results showed the interaction site between the peptides and the selected cell proteins (Original image are shown in Supplementary Figs. S6, S7, S8, S9, S10, S11, S12, S13, S14, S15, S16, S17).

regulation on Caspase3, yet MCF7 led to induce the apoptosis. These genes considered as tumour suppressors with a key role in cell cycle control and tumour progression. However, AtMP1 and AtMP2 significantly down-regulated the expression of antiapoptotic gene BCL-2 of MDA-MB-231 and MCF7 cells. Similarly, Murad and co-workers proved that the algal sulphated polysaccharide extract (ASPE) induces G1-phase arrest and apoptosis in MDA-MB-231 cells, which may serve as a potential therapeutic agent for breast cancer⁵¹. Another experimental result also found that the MCF7 cells are caspase-3 deficient with a partial deletion in the CASP-3 gene; these cells underwent cell death that lacked typical apoptotic properties⁵³. However, Nan et al. confirmed that caspase-3 serves a critical function in MCF7 cell, and they suggested that caspase-3 deficiency may contribute to the chemotherapy-resistance of breast cancer^{38,54}.

The extracted peptides of *A. testudineus* induced the cell death of MCF7 and MDA-MB-231 cells via the intrinsic apoptosis pathway, where the p53 expression led to the up-regulation of the pro-apoptotic gene BAX

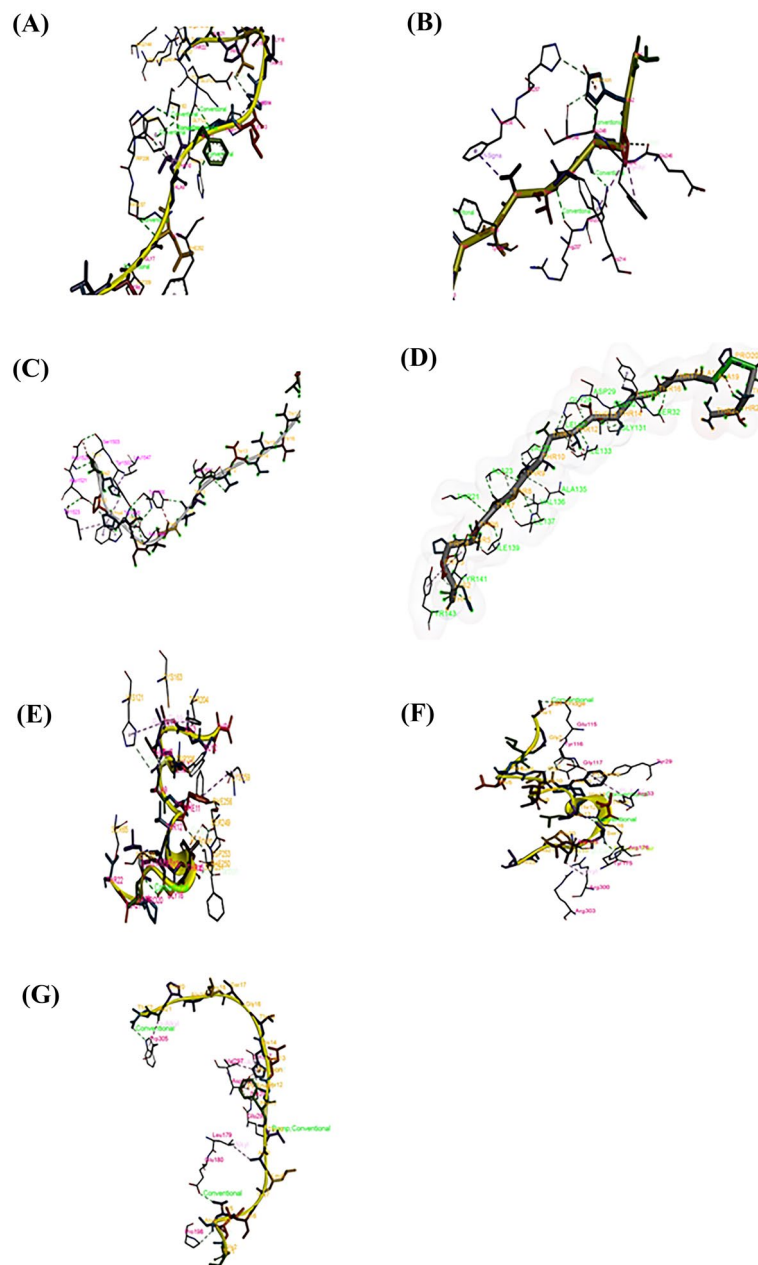
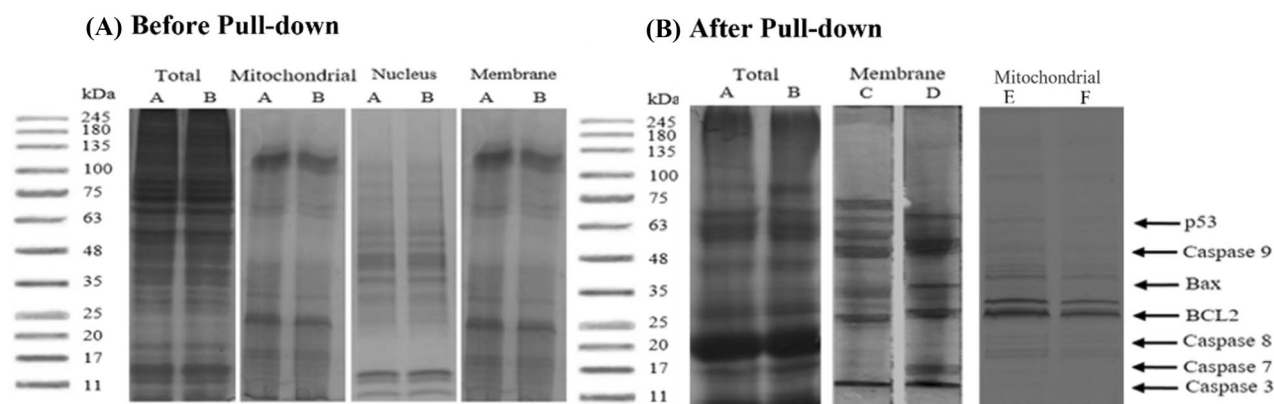


Figure 15. Peptide-protein docking 3D model by using ZDOCK. (A) AtMP2-BAX docking model, (B) AtMP2-caspase-3 docking model, (C) AtMP2-caspase-7 docking model, (D) AtMP2-Caspase8 docking model, (E) AtMP2-Caspase9 docking model, (F) AtMP2-P53 docking model, (G) AtMP2-BCL-2 docking model. The results showed the interaction site between the peptides and the selected cell proteins (original images are shown in Supplementary Figures S25, 26, 27, 28, 29, 30, 31).

and downregulation of the anti-apoptotic gene BCL-2. Leading to activate the executioner caspases (caspase-9, caspase-3, caspase-7, and caspase-8) and induced apoptosis. The proteins and peptides docking databases also proved the peptide-protein interaction. The result of proteins immunoprecipitation and the LC-MS analysis proves the validity of the findings of the proteins-peptides interaction prediction and RT² PCR analysis, which confirmed that AtMP1 and AtMP2 interact with tumour suppressor gene p53 and modulate the apoptosis-related proteins (caspase-9, caspase-3, caspase-7, caspase-8, p53, BCL2, and Bax), leading to induction of apoptosis and arrest the growth of breast cancer cell lines in G0/1 phase. These results were consistent with the findings reported by^{42,55,56}, which found that novel web servers, such as ZDOCK and HPEPDOCK, were useful for specific blind peptide-protein docking. Zhou et al. also confirmed that the HPEPDOCK could significantly predict the native global and local protein-peptide docking compared to other servers^{42,57}. This finding is in agreement with the previous studies stated that the antimicrobial peptide could inhibit the cancer cell line, such as Jurkat cells SCC-4 cell and MCF7, by modulating the expression of tumour suppressor gene p53 leading to activation



(C) list of protein detected by LC-MS

Uniprot ID	Gene Name	Score	MW
P14639	TP53	38	55 KDa
P42574	Caspase 3	36	20 KDa
P55210	Caspase 7	29	21 KDa
Q14790	Caspase 8	29	25 KDa
P55211	Caspase 9	27	50 KDa
Q07812	Bax	24	40 KDa

Figure 16. Peptide-protein immunoprecipitation analysis. (A) Total, membrane, and mitochondrial cell lysate before pulldown. (BA) total proteins linked to AtMP1 (BA) and (BB) total proteins linked to AtMP2 (BC) membrane proteins linked to AtMP1, and (BD) membrane proteins linked to AtMP2, and (BE) mitochondrial proteins linked to AtMP1, and (BF) mitochondrial proteins linked to AtMP1. (C) The list of cell proteins detected in LC-MS. (Gel blot figures are combination of different gels. The original pictures are shown in (Supplementary Figs. S18, S19, S20, S21, S22, S23, S24).

of pro-apoptotic gene Bax and inhibiting the anti-apoptotic gene BCL2^{56,58–61}. The result of proteins immunoprecipitation of the current study proves the validity of the findings of the proteins predictions analysis; which confirmed that AtMP1 and AtMP2 interact with tumour suppressor gene p53 and modulate the apoptosis-related proteins (caspase-3, 7, 8, 9, p53, BCL2, and Bax), leading to induction of apoptosis and arrest the growth of breast cancer cell lines in G0/1 phase.

In conclusion, the results described here clarify the fact that *A. testudineus* fish antimicrobial peptide functioned to inhibit MCF7 and MDA-MB-231 cells viability by inducing apoptosis. To the best of our knowledge, the present study is the first to reveal the exact mechanism of antimicrobial peptide extracted from *A. testudineus* fish mucus in the induction of MCF7 and MDA-MB-231 cell apoptosis. Therefore, the skin mucus of *A. testudineus* fish could be a notable source of a healing medicine interest toward human pathogens. This study provides a useful source for future research of cancer cell death and the change in genes that led to apoptosis, particularly in the MCF7 and MDA-MB-231 cell lines. However, the current study has tested the antimicrobial effect of *A. testudineus* peptides on two cancer cell line; further studies are required to examine the activity of antimicrobial peptides on several human cell lines and further characterization for these peptides' properties.

Received: 4 June 2021; Accepted: 9 November 2021

Published online: 30 November 2021

References

- Feng, Y. *et al.* Breast cancer development and progression: Risk factors, cancer stem cells, signaling pathways, genomics, and molecular pathogenesis. *Genes Dis.* **5**, 77–106 (2018).
- Siegel, R. L., Miller, K. D. & Jemal, A. Cancer statistics, 2020. *CA. Cancer J. Clin.* **70**, 7–30 (2020).
- Comşa, Ş, Cimpean, A. M. & Raica, M. The story of MCF-7 breast cancer cell line: 40 Years of experience in research. *Anticancer Res.* **35**, 3147–3154 (2015).
- Malve, H. Exploring the ocean for new drug developments: Marine pharmacology. *J. Pharm. Bioallied Sci.* **8**, 83–91 (2016).
- Yuan, H., Ma, Q., Ye, L. & Piao, G. The traditional medicine and modern medicine from natural products. *Molecules* **21**, 559 (2016).
- Buhari, I. & Roslida, A. Haruan fish extract as potential agent for cancer therapy. *J. Cancer Sci. Ther.* **7**(6), 186–189 (2016).
- Wei, O. Y., Xavier, R. & Marimuthu, K. Screening of antibacterial activity of mucus extract of snakehead fish, *Channa striatus* (Bloch). *Eur. Rev. Med. Pharmacol. Sci.* **14**(8), 675–681 (2010).

8. Shephard, K. L. Mucus on the epidermis of fish and its influence on drug delivery. *Adv. Drug Deliv. Rev.* **11**, 403–417 (1993).
9. Senevirathne, M. & Kim, S. K. *Development of Bioactive Peptides from Fish Proteins and Their Health Promoting Ability. Advances in Food and Nutrition Research* Vol. 65 (Elsevier Inc., 2012).
10. Jin, G. & Weinberg, A. Human antimicrobial peptides and cancer. *Semin. Cell Dev. Biol.* **88**, 156–162 (2019).
11. Urakova, I. N., Pozharitskaya, O. N., Demchenko, D. V., Shikov, A. N. & Makarov, V. G. The biological activities of fish peptides and methods of their isolation. *Russ. J. Mar. Biol.* **38**, 417–422 (2012).
12. Patrzykat, A., Gallant, J. W., Seo, J. K., Pytyck, J. & Douglas, S. E. Novel antimicrobial peptides derived from flatfish genes. *Anti-microb. Agents Chemother.* **47**, 2464–2470 (2003).
13. Kunda, N. K. Antimicrobial peptides as novel therapeutics for non-small cell lung cancer. *Drug Discov. Today* **25**, 238–247 (2020).
14. Wang, S. *et al.* Cell-in-cell death is not restricted by caspase-3 deficiency in MCF-7 cells. *J. Breast Cancer* **19**, 231–241 (2016).
15. Deslouches, B. & Di, Y. Antimicrobial peptides with selective antitumor mechanisms: Prospect for anticancer applications. *Oncotarget* **8**(28), 46635–46651 (2017).
16. Marqus, S., Pirogova, E. & Piva, T. J. Evaluation of the use of therapeutic peptides for cancer treatment. *J. Biomed. Sci.* **24**, 1–15 (2017).
17. Hsu, K. C., Li-Chan, E. C. Y. & Jao, C. L. Antiproliferative activity of peptides prepared from enzymatic hydrolysates of tuna dark muscle on human breast cancer cell line MCF-7. *Food Chem.* **126**, 617–622 (2011).
18. Lee, Y. *et al.* Peptides from anchovy sauce induce apoptosis in a human lymphoma cell (U937) through the increase of caspase-3 and -8 activities. *Ann. N. Y. Acad. Sci.* **1010**(1), 399–404 (2003).
19. Chen, J. Y., Lin, W. J. & Lin, T. L. A fish antimicrobial peptide, tilapia hepcidin TH2-3, shows potent antitumor activity against human fibrosarcoma cells. *Peptides* **30**, 1636–1642 (2009).
20. Chang, W. T., Pan, C. Y., Rajanbabu, V., Cheng, C. W. & Chen, J. Y. Tilapia (*Oreochromis mossambicus*) antimicrobial peptide, hepcidin 1–5, shows antitumor activity in cancer cells. *Peptides* **32**, 342–352 (2011).
21. Al-Rasheed, A. *et al.* Crude extracts of epidermal mucus and epidermis of climbing perch *Anabas testudineus* and its antibacterial and haemolytic activities. *Egypt. J. Aquat. Res.* **44**(2), 125–129 (2018).
22. Agarwal, S. K., Banerjee, T. & Mittal, A. A histochemical study of the epidermis of the climbing perch, *Anabas testudineus* (Anabantidae, Pisces). *Z. Mikrosk Anat Forsch* **94**(1), 143–159 (1980).
23. Dennison, S., Whittaker, M., Harris, F. & Phoenix, D. Anticancer & #945;-helical peptides and structure/function relationships underpinning their interactions with tumour cell membranes. *Curr. Protein Pept. Sci.* **7**, 487–499 (2006).
24. Tornesello, A. L., Borrelli, A., Buonaguro, L., Buonaguro, F. M. & Tornesello, M. L. Antimicrobial peptides as anticancer agents: Functional properties and biological activities. *Molecules* **25**, 2850 (2020).
25. Ross, N. W., Firth, K. J., Wang, A., Burka, J. F. & Johnson, S. C. Changes in hydrolytic enzyme activities of naive Atlantic salmon *Salmo salar* skin mucus due to infection with the salmon louse *Lepeophtheirus salmonis* and cortisol implantation. *Dis. Aquat. Organ.* **41**, 43–51 (2000).
26. Yang, J. Y. *et al.* Characteristics and emulsifying properties of two protein fractions derived from the emulsion formed during aqueous extraction of Camellia oil. *Food Hydrocoll.* **87**, 644–652 (2019).
27. Karpievitch, Y. V., Polpitiya, A. D., Anderson, G. A., Smith, R. D. & Dabney, A. R. Liquid chromatography mass spectrometry-based proteomics: Biological and technological aspects. *Ann. Appl. Stat.* **4**, 1797–1823 (2010).
28. Dong, G. F., Zheng, L., Huang, S. H., Gao, J. & Zuo, Y. C. Amino acid reduction can help to improve the identification of antimicrobial peptides and their functional activities. *Front. Genet.* **12**, 1–11 (2021).
29. Xiao, X., Wang, P., Lin, W. Z., Jia, J. H. & Chou, K. C. IAMP-2L: A two-level multi-label classifier for identifying antimicrobial peptides and their functional types. *Anal. Biochem.* **436**, 168–177 (2013).
30. Wagh, F. H., Barai, R. S., Gurung, P. & Idicula-Thomas, S. CAMPR3: A database on sequences, structures and signatures of antimicrobial peptides. *Nucleic Acids Res.* **44**, D1094–D1097 (2016).
31. Lee, H. T. *et al.* A large-scale structural classification of Antimicrobial peptides. *Biomed. Res. Int.* **2015**, 1–6 (2015).
32. Wang, G., Li, X. & Wang, Z. APD3: The antimicrobial peptide database as a tool for research and education. *Nucleic Acids Res.* **44**, D1087–D1093 (2016).
33. Balouiri, M., Sadiki, M. & Ibsouda, S. K. Methods for in vitro evaluating antimicrobial activity: A review. *J. Pharm. Anal.* **6**, 71–79 (2016).
34. Mohammed, F. A. *et al.* *Anethum graveolens* (dill)—A medicinal herb induces apoptosis and cell cycle arrest in HepG2 cell line. *J. Ethnopharmacol.* **219**, 15–22 (2018).
35. Mahmood, I. *et al.* Mutated Shiitake extracts inhibit melanin-producing neural crest-derived cells in zebrafish embryo. *Comp. Biochem. Physiol. Part C Toxicol. Pharmacol.* **245**, 109033 (2021).
36. Howard, T. P. *et al.* MDM2 and MDM4 are therapeutic vulnerabilities in malignant rhabdoid tumors. *Cancer Res.* **79**, 2404–2414 (2019).
37. Lee, P. Y., Costumbrado, J., Hsu, C. Y. & Kim, Y. H. Agarose gel electrophoresis for the separation of DNA fragments. *J. Vis. Exp.* <https://doi.org/10.3791/3923> (2012).
38. Wlodkowic, D., Skommer, J. & Darzynkiewicz, Z. Flow cytometry-based apoptosis detection. *Methods Mol. Biol.* **559**, 19–32 (2009).
39. Pierce, B. G. *et al.* ZDOCK server: Interactive docking prediction of protein–protein complexes and symmetric multimers. *Bioinformatics* **30**, 1771–1773 (2014).
40. Shai, Y. Mechanism of the binding, insertion and destabilization of phospholipid bilayer membranes by α -helical antimicrobial and cell non-selective membrane-lytic peptides. *Biochim. Biophys. Acta Biomembr.* **1462**, 55–70 (1999).
41. Berman, H. M. *et al.* The protein data bank. *Nucleic Acids Res.* **28**, 235–242 (2000).
42. Zhou, P., Jin, B., Li, H. & Huang, S. Y. HPEPDOCK: A web server for blind peptide–protein docking based on a hierarchical algorithm. *Nucleic Acids Res.* **46**, W443–W450 (2018).
43. Kulkarni, S. A. *et al.* Computational evaluation of major components from plant essential oils as potent inhibitors of SARS-CoV-2 spike protein. *J. Mol. Struct.* **1221**, 128823 (2020).
44. Zhu, Y. Y., Huang, H. Y. & Wu, Y. L. Anticancer and apoptotic activities of oleanolic acid are mediated through cell cycle arrest and disruption of mitochondrial membrane potential in HepG2 human hepatocellular carcinoma cells. *Mol. Med. Rep.* **12**, 5012–5018 (2015).
45. Cheah, J. S. & Yamada, S. A simple elution strategy for biotinylated proteins bound to streptavidin conjugated beads using excess biotin and heat. *Biochem. Biophys. Res. Commun.* **493**, 1522–1527 (2017).
46. E-Kobon, T., Thongararm, P., Roytrakul, S., Meesuk, L. & Chumnanpuen, P. Prediction of anticancer peptides against MCF-7 breast cancer cells from the peptidomes of *Achatina fulica* mucus fractions. *Comput. Struct. Biotechnol. J.* **14**, 49–57 (2016).
47. Rozek, T. *et al.* The antibiotic and anticancer active aurein peptides from the Australian Bell Frogs *Litoria aurea* and *Litoria raniiformis*: The solution structure of aurein 1.2. *Eur. J. Biochem.* **267**, 5330–5341 (2000).
48. Kuo, H.-M. *et al.* MSP-4, an antimicrobial peptide, induces apoptosis via activation of extrinsic Fas/FasL- and intrinsic mitochondria-mediated pathways in one osteosarcoma cell line. *Mar. Drugs* **16**, 8 (2018).
49. Rakers, S. *et al.* Antimicrobial peptides (AMPs) from fish epidermis: Perspectives for investigative dermatology. *J. Investig. Dermatol.* **133**, 1140–1149 (2013).
50. Gaspar, D., Freire, J. M., Pacheco, T. R., Barata, J. T. & Castanho, M. A. R. B. Apoptotic human neutrophil peptide-1 anti-tumor activity revealed by cellular biomechanics. *Biochim. Biophys. Acta Mol. Cell Res.* **1853**, 308–316 (2015).

51. Murad, H. *et al.* Induction of G1-phase cell cycle arrest and apoptosis pathway in MDA-MB-231 human breast cancer cells by sulfated polysaccharide extracted from *Laurencia papillosa*. *Cancer Cell Int.* **16**, 1–11 (2016).
52. Li, Y., Upadhyay, S., Bhuiyan, M. & Sarkar, F. H. Induction of apoptosis in breast cancer cells MDA-MB-231 by genistein. *Oncogene* **18**, 3166–3172 (1999).
53. Wang, S., Wang, Y., Ma, J., Ding, Y. & Zhang, S. Phosvitin plays a critical role in the immunity of zebrafish embryos via acting as a pattern recognition receptor and an antimicrobial effector. *J. Biol. Chem.* **286**, 22653–22664 (2011).
54. Nan, M. L. *et al.* Rotundic acid induces Cas3-MCF-7 cell apoptosis through the p53 pathway. *Oncol. Lett.* **17**, 630–637 (2019).
55. Ciemny, M. P., Kurcinski, M., Blaszczyk, M., Kolinski, A. & Kmiecik, S. Modeling EphB4-EphrinB2 protein–protein interaction using flexible docking of a short linear motif. *Biomed. Eng. Online* **16**, 137–145 (2017).
56. Shahid, M. *et al.* Comprehensive computational target fishing approach to identify Xanthorrhizol putative targets. *Sci. Rep.* **11**, 1–11 (2021).
57. Chen, J. The cell-cycle arrest and apoptotic functions of p53 in tumor initiation and progression. *Cold Spring Harb. Perspect. Med.* **6**(3), a026104 (2016).
58. Alijani Ardeshir, R. *et al.* Selective induced apoptosis and cell cycle arrest in MCF7 and LNCap cell lines by skin mucus from round goby (*Neogobius melanostomus*) and common carp (*Cyprinus carpio*) through P53 expression. *Cytotechnology* **72**, 1–10 (2020).
59. Lima, Z. S. *et al.* Recent advances of therapeutic targets based on the molecular signature in breast cancer: Genetic mutations and implications for current treatment paradigms. *J. Hematol. Oncol.* **12**, 1–25 (2019).
60. Zhu, Y. *et al.* Intra-S-phase checkpoint activation by direct CDK2 inhibition. *Mol. Cell. Biol.* **24**, 6268–6277 (2004).
61. Arockiaraj, J. *et al.* Crustin, a WAP domain containing antimicrobial peptide from freshwater prawn *Macrobrachium rosenbergii*: Immune characterization. *Fish Shellfish Immunol.* **34**, 109–118 (2013).

Acknowledgements

This study was supported by Universiti Kebangsaan Malaysia, Grant no. DCP-2018-006/1.

Author contributions

A.A.N. and S.F. contributed to the acquisition of data and writing the first version of the manuscript. A.A., M.S. and N.K. revised the manuscript for essential intellectual content. H.R.E.D., S.S., and B.A.O. drafting and revising the manuscript, and coordinated the project. All authors approved the final version of the manuscript.

Competing interests

The authors declare no competing interests.

Additional information

Supplementary Information The online version contains supplementary material available at <https://doi.org/10.1038/s41598-021-02007-6>.

Correspondence and requests for materials should be addressed to S.F.

Reprints and permissions information is available at www.nature.com/reprints.

Publisher's note Springer Nature remains neutral with regard to jurisdictional claims in published maps and institutional affiliations.



Open Access This article is licensed under a Creative Commons Attribution 4.0 International License, which permits use, sharing, adaptation, distribution and reproduction in any medium or format, as long as you give appropriate credit to the original author(s) and the source, provide a link to the Creative Commons licence, and indicate if changes were made. The images or other third party material in this article are included in the article's Creative Commons licence, unless indicated otherwise in a credit line to the material. If material is not included in the article's Creative Commons licence and your intended use is not permitted by statutory regulation or exceeds the permitted use, you will need to obtain permission directly from the copyright holder. To view a copy of this licence, visit <http://creativecommons.org/licenses/by/4.0/>.

© The Author(s) 2021